KU LEUVEN

FACULTY OF SCIENCE

Schwinger effect in Reissner-Nordström-de Sitter spacetime

Ben WILLEBRORDS

Supervisor: prof. dr. T. Van Riet
KU Leuven

Thesis presented in
fulfillment of the requirements
for the degree of Master of Science
in Physics

Academic year 2024-2025

Contents

Foreword

Nothing in this universe is undeserving of a physicist's curiosity and attention. But, naturally, some topics are more appealing than others according to one's own taste. Personally, I was very happy when it turned out that I could use this master's thesis project to take a deep dive into the interplay between gravity and quantum fields. Black holes remain some of the most confusing, mysterious and scary objects out there (more than one night's sleep has been filled with the dream of falling into one), but I consider it a privilege to have been given the time and guidance to get to know them just a little bit better.

Although a master's thesis is written alone, it is not an individual undertaking. Consequently, there are many people to thank for their help and support during the process. First of all, my utmost appreciation goes out to my supervisor, prof. Thomas Van Riet. After this thesis project had taken a couple of false starts at the beginning of the academic year, Thomas was extremely kind to immediately take over as supervisor and advise me on physics and possible career choices.

Secondly, I wish to thank my fellow students in the Master of Physics, especially those with whom I shared an office on the sixth floor of building D, for embracing a wandering philosopher as one of their own.

Thirdly, thank you to my friends and family, including my mother, brother, sister, and lovely tiny nephews and nieces, for ever reminding me that moving, self-replicating clumps of matter are more than the sum of their constituents.

And finally, to my fiancée Rune, for her unwavering support throughout the last two years and for our occasional conversational travels to the stars, I owe an amount of gratitude so large that it is at danger of collapsing into a black hole. Thank you, Rune, for being the awesome, intelligent, happy, sweet, beautiful person you are.

Contribution statement

The results in Chapter 1 are mainly taken from [9, 55]. Chapter 2 is a reconstruction of [37]. Chapter 3 is based on [40]. The calculations presented in Chapter 4 were performed by the author of this work.

Scientific summary

The Schwinger effect is the phenomenon whereby charged particle-antiparticle pairs are spontaneously produced in the presence of an electric field, and constitutes one channel through which charged black holes can lose their charge and evaporate. This thesis is a study of the Schwinger effect around charged black holes embedded in de Sitter space. These spacetimes sport three horizons: two for the black hole and a cosmological one for de Sitter space. In this dissertation, we will be mostly interested in the extremal and Nariai limits of these spacetimes, in which two of the three horizons coincide. If there exists a charged particle species with a sufficiently small mass, the Schwinger effect becomes so violent that it leaves behind a pathological spacetime exhibiting a Big Crunch. One way to prevent this scenario is to ensure that the Schwinger effect cannot become explosive by adopting the *Festina Lente* bound, a bound on the charge-to-mass ratio of particles.

However, some authors have raised doubts about the assumptions that go into the derivation of the Festina Lente bound. Therefore, we wish to get a better understanding of the spatial profile of the Schwinger effect around a charged black hole embedded in a de Sitter background, since understanding the interaction of the produced particle-antiparticle pairs with the cosmological horizon may be key to evaluating the validity of the Festina Lente proposal. In this thesis, we use the worldline formalism to calculate the instanton action and, in doing so, make a contribution towards a better understanding of the spatial profile of the Schwinger effect in these spacetimes.

First, we give a general introduction to quantum field theory in curved spacetime. We pay special attention to how changing gravitational fields can give rise to the spontaneous creation of particles and use instantons to derive the Hawking effect in Schwarzschild spacetime. Next, we give a derivation of the Schwinger effect in Minkowski spacetime and develop the worldline formalism, which we then use to derive the Schwinger effect around a charged black hole. After that, we place the black hole in a de Sitter background and investigate how it evolves under the influence of the Schwinger effect; we analyse in some detail the derivation that leads to the Festina Lente bound. Finally, we extend the worldline algorithm to these de Sitter black holes. As it turns out, the algorithm performs well when applied to small extremal black holes, validating our approach in that corner of parameter space. However, the algorithm shows questionable behaviour when applied to large extremal black holes, in which case it predicts a dramatically enhanced Schwinger effect near the cosmological horizon, and fails to produce results on the charged Nariai branch. Both problems are probably due to numerical instabilities. We give suggestions for how to make the implementation of the numerical solver more robust in future work.

Summary for a general audience

This thesis explores how black holes can lose their electric charge by creating particles out of empty space. This process, called the Schwinger effect, occurs when powerful electric fields near a black hole cause pairs of particles to suddenly appear. It is one of the ways black holes gradually fade away.

The work focusses on black holes that exist in a universe with a positive cosmological constant, known as de Sitter space. In this environment, there are three different 'horizons', that is, boundaries in space and time beyond which information is irretrievably lost. The study pays special attention to situations where two of these horizons overlap.

If certain types of particles exist with just the right properties, the Schwinger effect can become so violent that it destabilises space itself, ending in a catastrophic collapse (a 'Big Crunch'). To avoid this, physicists have proposed a safeguard known as the Festina Lente bound, which limits the types of particles that can exist. However, some researchers question whether the assumptions behind this safeguard are reliable.

This thesis aims to improve our understanding of how the Schwinger effect works around charged black holes in de Sitter space, particularly near the cosmological horizon. Using advanced mathematical tools, the research calculates how particle creation behaves in different scenarios. The results suggest that the method works well for smaller black holes, but for larger ones, the predictions become unstable, pointing to areas where future improvements in the calculations are needed.

In short, this work contributes to a deeper understanding of how black holes lose their charge, how particle creation interacts with the universe's expansion, and whether the proposed safeguards against cosmic collapse hold up under closer examination.

List of abbreviations and symbols

Abbreviations

(A)dS	(Anti-)de Sitter spacetime
AF	Asymptotically flat spacetime
FL	Festina Lente
QED	Quantum electrodynamics
RN(dS)	Reissner-Nordström(-de Sitter) spacetime
WCCC	Weak cosmic censorship conjecture
QFT(CS)	Quantum field theory (in curved spacetime)

Symbols

$\Box$	d'Alembertian
$\mathrm{d}\Omega_2^2$	Metric on 2-sphere
$\hbar$	Reduced Planck constant
∇	Covariant derivative
A	Electromagnetic four-potential
c	Speed of light in vacuum
F	Electromagnetic field strength tensor
G	Universal constant of gravitation
$g_{\mu\nu}$	Spacetime metric
R	Ricci scalar
S	Action
z	Charge-to-mass ratio

“Rien, mais rien qui ne soit vraiment rien.”
— Paul Nougé, *L’expérience continue*

Introduction

It does not seem unfair to say that understanding black holes is the key to understanding physics at its most fundamental level. With their dramatic curving of spacetime and intricate interactions with quantum fields, black holes are right there at the edge of our knowledge, even more than a hundred years after their prediction on the basis of the general theory of relativity. In recent years, the scientific community has learnt many new things about them and has discovered a few new methods of doing so, the most groundbreaking being the detection and analysis of gravitational waves [2]. It is near-certain that the coming years will provide physicists with novel and interesting observational black hole data.

However, our universe probably only supports certain classes of black holes, namely stationary and rotating massive black holes. Charged black holes form a different class of black holes that could theoretically exist but are not expected to exist in our universe. The reason why is that matter in our universe is typically clumped together to have a zero net electric charge, which makes it hard for black holes to become charged in the first place. Moreover, even if we were to try and give an existing black hole charge artificially (for example by shooting it with a ray of electrons or protons) it would be difficult to give it a truly considerable charge, since our charged projectiles would become more and more repulsed by the black hole as it is charged up. Consequently, there exists an entire class of fascinating black holes that we should not expect to observe in real life anytime soon (cf. [12] for a rather entertaining discussion of the prospects for using highly charged black holes as a laboratory for observing the effects of quantum gravity).

We can be saddened by this a little, but not too much. Surely, there is more to science than only observing and modelling. Imagination is, arguably, just as important to the scientific method as these other, more talked-about aspects of it. Especially since new results in fundamental physics are hard to come by these days, we should not dismiss any instrument in our toolbox as being unorthodox, as long as we have the faintest hope that it could help us move our investigations further along. As such, charged black holes can play an important role in thought experiments and theoretical studies. For example, theoretical charged black holes have the feature that there is an upper bound on how much charge they can hold relative to their mass. If this threshold is exceeded, the black hole loses its horizon, effectively becoming a naked singularity [14]. There is reason to believe that the existence of naked singularities would be problematic, leading physicists to postulate that Nature should be such that their formation is in some way prevented [61, 66]. Hence, charged black holes can be a source of information about Nature, even if they are not observable in our universe.

Charged black holes can be embedded in a variety of background spacetimes. The background we will be most concerned with in this dissertation is the positively curved

and expanding de Sitter spacetime. If a charged black hole is placed in a de Sitter universe, the resulting spacetime sports three horizons: two for the black hole and a cosmological one for de Sitter space. In the most extreme cases, two or three of these horizons can coincide [57]; these extreme cases are the ones that we will be interested in in this thesis. When black holes are allowed to interact with the quantum fields permeating the spacetimes, they will evaporate. In the case of an uncharged black hole, this process is called Hawking radiation [33]; in the case of a large charged black hole, the dominant mechanism of evaporation is the Schwinger effect [26]: the electric field set up by the charge of the black hole causes the production of charged particle-antiparticle pairs out of the vacuum, which depletes the black hole of its charge and mass [60].

Interestingly, in the case of a charged black hole in de Sitter for which the outer black hole horizon coincides with the cosmological horizon, the evaporation can in some cases be so violent that it leaves behind a pathological spacetime exhibiting a Big Crunch. This seems like a scenario that Nature should in some way avoid, similar to the prevention of naked singularities. One way to do this is to ensure that the Schwinger effect cannot become too explosive by placing a bound, dubbed the *Festina Lente* bound, on the charge-to-mass ratio of particles [40]. In essence, contemplating the scenario of exploding degenerate charged black holes in de Sitter teaches us something about particle phenomenology.

However, some authors have raised doubts about the assumptions that went into the derivation of the Festina Lente bound [1, 37]. To take these worries seriously means either to give a clear reason why the assumptions that led to the Festina Lente bound are not appropriate for describing the evaporation of the charged black hole under question, or to show that the Festina Lente bound is a robust prediction by re-deriving it through different means. In this thesis, we will make a contribution towards the second option. Concretely, we wish to get a better understanding of the spatial profile of the Schwinger effect around a charged black hole embedded in a de Sitter background, since understanding the interaction of the produced particle-antiparticle pairs with the cosmological horizon may be key to evaluating the validity of the Festina Lente proposal. To do so, we will extend to a de Sitter background an algorithm first applied to charged black holes in a flat background by [37].

This thesis will be structured as follows. In Chapter 1, we will give a general introduction to the field of quantum field theory in curved spacetime. We pay special attention to how changing gravitational fields can give rise to the production of particles, and, as a culmination of this first chapter, we will use instantons to derive the Hawking effect in Schwarzschild spacetime. Next, in Chapter 2, we will give a derivation of the Schwinger effect in Minkowski spacetime and develop a formalism to derive the Schwinger effect around charged black holes in a flat background. Then, in Chapter 3, we place a charged black hole in de Sitter spacetime, dissect its geometry, and investigate how it evolves under the influence of the Schwinger effect. Here, we will in some detail analyse the Festina Lente bound, how it is derived, and how it fits into the larger picture of the swampland programme. Finally, in Chapter 4, we extend the machinery we had previously developed in Chapter 2 to charged black holes in a de Sitter background. As we shall see, the algorithm performs well when applied to relatively small extremal black holes but shows questionable behaviour when applied to large extremal black holes or Nariai black holes.

Chapter 1

Quantum effects in curved spacetime

Introduction

The general theory of relativity is a theory of the geometry of space and time, and as such gives an excellent description of the gravitational phenomena in our universe, including the orbits of planets, the expansion of the universe, and the existence of gravitational waves. Nevertheless, there are also aspects of gravity that are currently unexplained by general relativity, such as the nature of dark matter, dark energy, and spacetime singularities. Although firmly rooted in modern physics, general relativity is a *classical* theory, meaning that it does not incorporate quantum theory. However, there is reason to believe that to give a full account of gravity, one requires a new theory, a so-called theory of *quantum gravity*, in which gravity and the other forces are placed on an equal footing.[1] String theory and loop quantum gravity are just two examples of theories of quantum gravity, of which string theory is at present the dominant paradigm.

However, instead of diving headlong into the search for a theory of quantum gravity, it can be interesting to see how far one can go in fusing general relativity and quantum theory before quantising gravity. In the case where the spacetime is Minkowski spacetime, the combination with quantum theory results in quantum field theory (QFT). The study of QFT led to the formulation of the Standard Model of particle physics, a description of the electroweak and strong forces in Nature, and one of the most accurately tested theories in all of science. The Earth's gravitational field is weak enough to justify a flat spacetime approximation for experiments conducted at CERN, but at the end of the day, most spacetimes of interest (including our own) are quite obviously not a Minkowski spacetime. Studying quantum theory in spacetimes beyond Minkowski results in quantum field theory in curved spacetime (QFTCS).

QFTCS, like QFT, is a semi-classical theory: the matter and energy content of the spacetime are treated quantum-mechanically, whereas the spacetime itself is treated in a classical, relativistic way. In other words, backreactions from quantum fields on the spacetime are neglected. Surprisingly, even at the level of linearized, free theories in QFTCS, the coupling of quantum fields to the geometry of spacetime gives rise to new phenomena not present in regular QFT. The most famous example of such a phenomenon is the emis-

[1] At a foundational level, the reason why we need a theory of quantum gravity is that semi-classical theories suffer from a loss of unitarity. Plainly said, semi-classical theories leak probability [15]. This means that in regions of spacetime where backreactions of quantum fields on the spacetime become important, some physical phenomena are almost certainly not explained by our current theories.

sion of radiation by black holes, a process through which black holes are expected to lose mass and ultimately evaporate away. This effect is called *Hawking radiation* and is not derivable from general relativity alone. Another important prediction of QFTCS is the production of particles in the early inflationary universe, a probable source of the perturbations that gave rise to the anisotropies in the cosmic microwave background observed today. As a final example, QFTCS predicts that an accelerating observer in Minkowski spacetime will observe so-called *Unruh radiation*, much like an observer near a black hole is expected to observe Hawking radiation. (Although technically, the Unruh effect is a quantum effect in Minkowski spacetime, it shows a lot of similarities with Hawking radiation and is therefore often discussed in the context of QFTCS.)

There is little reason to believe that the spacetime that is the main object of study of this thesis, namely a Reissner-Nordström black hole in a de Sitter universe, exists in Nature in any appreciable form — let alone the extremal limits of this spacetime. Consequently, one should not expect this type of black hole to be observed anytime soon. However, studying this spacetime is interesting from a theoretical point of view. Even though QFTCS is not a theory of quantum gravity, it is expected to be a low-energy limit of a theory that is valid at high energies. This insight can be used in either of two ways. Either results from the low-energy theory can be used to constrain theories at higher energies, or the low-energy theory can be constrained through the demand that it should be able to be consistently incorporated into a theory of quantum gravity at high energies. In this thesis, we will approach Reissner-Nordström-de Sitter black holes from these points of view.

This chapter will be structured as follows. In Section 1.1, we will briefly discuss the most elementary black hole model in the context of general relativity, namely the Schwarzschild black hole. In Section 1.2, we will consider some general aspects of quantum field theory in curved spacetime, with special attention to the relativity of the vacuum and particle production in changing gravitational fields. Finally, in Section 1.3, we will demonstrate how such particle production manifests itself in the Schwarzschild spacetime, leading to a derivation of Hawking radiation through the use of instantons.

1.1 Schwarzschild black holes in general relativity

Black holes are probably some of the most awe-inspiring objects in physics, both for the working physicist and for the general public. Interestingly, they are characterized by at most three parameters (mass, charge, and angular momentum), making them some of the simplest physical objects imaginable while still giving rise to a plethora of fascinating phenomena and paradoxes. Each black hole has an event horizon (barring the possibility of *naked singularities*, discussed in Section 2.1). A black hole's event horizon is a radius from the centre of the black hole that functions as a 'point of no return': once matter crosses the event horizon, it can only keep moving in the direction of the singularity at the black hole's centre. In other words, matter falling into a black hole cannot come out again (at least not in any recognizable way, raising questions about the implications of the existence of black holes for the conservation of information [53, 54]). Famously, this also includes light. As a result, the horizon divides the spacetime into distinct causal regions: the region outside of the event horizon can influence events on the inside, but not the other way around. Specific species of black holes can have additional horizons (cf.

Section 2.1).

Black holes are among the densest objects in the universe. It was shown by Penrose in 1965 that the formation of black holes through gravitational collapse is a solid prediction of the general theory of relativity [49], and the existence of astrophysical black holes has been confirmed through multiple observations. The first evidence came in the form of observations of the orbits of stars near the centre of the Milky Way, which allowed astronomers to infer that our galaxy harbours a massive central black hole [25, 29]. Penrose's prediction, together with Ghez's and Genzel's observations, led to their being awarded the 2020 Nobel Prize in Physics. The second confirmation of the existence of black holes reached Earth in the form of gravitational waves. The existence of gravitational waves was inferred from the general theory of relativity by Einstein in 1916 [21]. Whenever extremely massive, dense objects (such as black holes and neutron stars) spiral into each other, collide, and become one new object, they create waves propagating in spacetime that, given that they are strong enough, can be observed. The first observation of gravitational waves occurred in 2015 by the LIGO collaboration [2], which resulted in the Nobel Prize in Physics of 2017 being awarded to Weiss, Barish, and Thorne. Thirdly, through a technique called very-long-baseline interferometry, the Event Horizon Telescope collaboration has been able to image black holes directly [4]. Other evidence is provided by the observation of accretion disks around black holes and gravitational microlensing.

The simplest black hole solution to the Einstein field equations is the Schwarzschild black hole, a massive yet uncharged and non-rotating black hole whose exterior is well described by the metric

$$\mathrm{d}s^2 = -\left(1 - \frac{2GM}{c^2 r}\right)\mathrm{d}t^2 + \left(1 - \frac{2GM}{c^2 r}\right)^{-1}\mathrm{d}r^2 + r^2\,\mathrm{d}\Omega_2^2, \tag{1.1}$$

where $\mathrm{d}\Omega_2^2$ is the metric on the unit two-sphere,

$$\mathrm{d}\Omega_2^2 = \mathrm{d}\theta^2 + \sin^2\theta\,\mathrm{d}\varphi^2, \tag{1.2}$$

and where M is the black hole's constant mass.

The Schwarzschild spacetime seemingly contains two singularities: one for $r = 0$ and a second for $r = 2GM/c^2$. However, through a suitable coordinate transformation (such as to Kruskal-Szekeres coordinates), one can show that $r = 2GM/c^2$ is only a coordinate singularity and, in fact, corresponds to the black hole's event horizon. On the other hand, the singularity for $r = 0$ is a gravitational singularity and cannot be removed in this way.

For our purposes, it is important to note two extra features of the Schwarzschild spacetime. First, there is no a priori limit on how big a Schwarzschild black hole can be; its mass M and consequently its Schwarzschild radius $2GM/c^2$ are in principle unbounded. Secondly, an observer moving radially away from the black hole will notice the gravitational influence of the black hole diminish, and the spacetime around her will start to look more and more like Minkowski spacetime. This can also be seen from Eq. 1.1: in the limit $r \to \infty$, the Schwarzschild metric becomes

$$\mathrm{d}s^2 = -\,\mathrm{d}t^2 + \mathrm{d}r^2 + r^2\,\mathrm{d}\Omega_2^2, \tag{1.3}$$

which is precisely the Minkowski metric. Whenever a spacetime becomes Minkowski at radial infinity, the spacetime is said to be *asymptotically flat*. An example of a spacetime that is not asymptotically flat is de Sitter spacetime, as we will see in Chapter 3. Henceforth, we will work in a geometrised unit system ($G = c = 1$).

1.2 Quantum field theory in curved spacetime

We now discuss some preliminary aspects of QFTCS, thereby setting the stage for our discussion of Hawking radiation in Schwarzschild spacetime. Our discussion will be based on [9, 55].

1.2.1 Quantising a real scalar field

Consider a real massive scalar field $\phi(x)$ in a globally hyperbolic[2] four-dimensional spacetime, described by the action

$$S = -\frac{1}{2}\int \mathrm{d}^4x\,\sqrt{-g}\left[g^{\mu\nu}\partial_\mu\phi\partial_\nu\phi + \left(m^2+\xi R\right)\phi^2\right], \tag{1.4}$$

where $g_{\mu\nu}(x)$ is the (mostly plus) spacetime metric, $g(x)$ is its determinant, m is the field quanta's mass, ξ is the coupling of the scalar field to the gravitational field, and $R(x)$ is the spacetime's Ricci scalar. Application of the principle of stationary action results in a curved spacetime analog of the Klein-Gordon equation:

$$\left[\Box - m^2 - \xi R(x)\right]\phi(x) = 0, \tag{1.5}$$

with the d'Alembert operator $\Box$ defined in terms of the covariant derivative ∇:

$$\Box = g^{\mu\nu}\nabla_\mu\nabla_\nu. \tag{1.6}$$

Since Eq. 1.5 is a linear equation, its solutions will have the structure of a vector space, which we denote by $\mathcal{S}$. We then define a form $(\cdot,\cdot)$ on $\mathcal{S}$ by

$$(\alpha,\beta) = i\int_\Sigma \mathrm{d}\Sigma\, n^\mu\sqrt{h}\left[\alpha^*\nabla_\mu\beta - \beta\nabla_\mu\alpha^*\right], \tag{1.7}$$

where Σ is a Cauchy hypersurface of the spacetime, $\mathrm{d}\Sigma$ is its volume element, n^μ is a future-oriented unit vector orthogonal to Σ, and $h_{ij}(x)$ is the induced metric on Σ. It can be shown quite easily that the quantity between brackets in Eq. 1.7 is conserved and thus that $(\cdot,\cdot)$ is independent of the choice of surface Σ. Importantly, the product defined by Eq. 1.7 is not a scalar product, since it is not positive definite. In other words, $(\mathcal{S},(\cdot,\cdot))$ is not a normed vector space.[3] However, we can always decompose $\mathcal{S}$ into two orthogonal subspaces $\mathcal{S}_p$ and $\mathcal{S}_p^*$ such that $(\cdot,\cdot)$ is positive definite on both subspaces and such that and $\mathcal{S} = \mathcal{S}_p \oplus \mathcal{S}_p^*$.

Now, let $\{u_\lambda(x)\}$ be a complete and orthonormal set of solutions in $\mathcal{S}_p$. Then $\{u_\lambda^*(x)\}$ is a complete and orthonormal set of solutions in $\mathcal{S}_p^*$. The field ϕ can then be expanded as a linear combination of solutions in $\mathcal{S}$:

$$\phi = \int \mathrm{d}\mu(\lambda)\left[a_\lambda u_\lambda + a_\lambda^\dagger u_\lambda^*\right], \tag{1.8}$$

[2] A spacetime is called globally hyperbolic if it allows for a foliation into Cauchy hypersurfaces. A Cauchy hypersurface is a hypersurface of the spacetime in which no two points are connected by a non-spacelike curve (i.e. a curve whose tangent vector is not everywhere spacelike).

[3] To be precise, $(\cdot,\cdot)$ is a sesquilinear form over the complex vector space $\mathcal{S}$, whose defining property is that it is anti-linear in its first argument and linear in its second.

where

$$a_\lambda = (u_\lambda, \phi), \quad a_\lambda^\dagger = -(u_\lambda^*, \phi). \tag{1.9}$$

Next, we quantise the theory by interpreting a and $a^\dagger$ as annihilation and creation operators respectively and imposing the canonical commutation relations

$$\left[a_{\lambda_1}, a_{\lambda_2}^\dagger\right] = \delta(\lambda_1 - \lambda_2), \quad \left[a_{\lambda_1}, a_{\lambda_2}\right] = \left[a_{\lambda_1}^\dagger, a_{\lambda_2}^\dagger\right] = 0. \tag{1.10}$$

With these operators in hand, we then proceed to define a vacuum state $|0_u\rangle$ by

$$\forall u_\lambda \in \mathcal{S}_p : a_\lambda |0_u\rangle = 0, \quad \langle 0_u | 0_u \rangle = 1. \tag{1.11}$$

The n-particle states are built from the vacuum as

$$a_{\lambda_1}^\dagger a_{\lambda_2}^\dagger \dots a_{\lambda_n}^\dagger |0_u\rangle. \tag{1.12}$$

We can also define the number operator

$$N_\lambda = a_\lambda^\dagger a_\lambda, \tag{1.13}$$

which counts the number of particles associated with the mode u_λ in a given state.

1.2.2 Vacua and particles

Note how the definition of the creation and annihilation operators in Eq. 1.9 is crucially dependent on the choice of mode decomposition of $\mathcal{S}$. Not only that, there is also no way to decide which decomposition of $\mathcal{S}$, and thus which representation of the canonical commutation relations, is the 'right' or 'preferred' one. This is due to the breakdown of the Stone-von Neumann theorem in quantum field theory. The Stone-von Neumann theorem ensures the unitary equivalence of different representations of the canonical commutation relations in quantum systems with finitely many degrees of freedom, but it does not hold in systems with infinitely many degrees of freedom. In other words, the theorem holds in quantum mechanics, but not in quantum field theory [65].

This is also true for QFT in flat spacetime. However, in Minkowski spacetime, there is a loophole. Due to the presence of the timelike Killing vector ∂_t, a 'natural' decomposition of $\mathcal{S}$ into so-called *positive* and *negative* frequency solutions is possible. Generic spacetimes will not have a timelike Killing vector and thus no preferred mode decomposition (but if they do happen to have such symmetries, this usually simplifies things significantly). The absence of Poincaré invariance in generic spacetimes thus means that different inertial observers will not agree on the choice of vacuum, and since the counting of particles is based on the definition of the vacuum, different observers will disagree on how many particles are present. It is precisely this disagreement that leads to the fascinating distinctive phenomena in QFTCS. (Note that the specification *inertial* is crucial here: even in Minkowski spacetime, an accelerating observer will not agree with an inertial observer on the choice of vacuum, giving rise to the Unruh effect.) From a philosophical point of view, the particle interpretation of quantum fields becomes ambiguous (even more than it already was in quantum mechanics) and may lose its meaning entirely.[4]

[4] A formulation of QFT more satisfying than the canonical quantisation formulation can be found in the framework of algebraic quantum field theory, which successfully singles out the invariant aspects of QFTCS and thus circumvents issues with the particle interpretation (cf. [65]).

1.2.3 Particle production in a time-dependent gravitational field

To show that a different construction gives rise to a different vacuum, consider the following scenario. A globally hyperbolic spacetime is approximately stationary at early times, evolves in a non-stationary way at middle times, and becomes stationary again at late times. Stationarity implies the existence of a timelike Killing vector and thus the existence of a 'preferred' decomposition of $\mathcal{S}$. Let $\mathcal{S} = \mathcal{S}_p \oplus \mathcal{S}_p^*$ be the appropriate decomposition for the spacetime at early times, with $\{u_\lambda(x)\} \subset \mathcal{S}_p$ a complete and orthonormal set of solutions. Similarly, let $\mathcal{S} = \mathcal{S}_p' \oplus \mathcal{S}_p'^*$ be the appropriate decomposition for the spacetime at late times, with a complete and orthonormal set of solutions $\{w_\kappa(x)\} \subset \mathcal{S}_p'$. As before, we can expand ϕ as

$$\phi = \int \mathrm{d}\mu(\kappa) \left[b_\kappa w_\kappa + b_\kappa^\dagger w_\kappa^* \right], \tag{1.14}$$

where we again identify b and $b^\dagger$ as annihilation and creation operators. The vacuum is now defined by

$$\forall w_\kappa \in \mathcal{S}_p : b_\kappa |0_w\rangle = 0, \quad \langle 0_w | 0_w \rangle = 1 \tag{1.15}$$

and we can again build multi-particle states from this vacuum.

Like we can expand ϕ in both bases, we can expand the basis vectors of one basis in terms of the other basis. These expansions can be shown to satisfy the *Bogoliubov transformations*

$$\begin{cases} u_\lambda = \int \mathrm{d}\mu(\kappa) \left[A_{\kappa\lambda}^* w_\kappa - B_{\kappa\lambda} w_\kappa^* \right] \\ w_\kappa = \int \mathrm{d}\mu(\lambda) \left[A_{\kappa\lambda} u_\lambda + B_{\kappa\lambda} u_\lambda^* \right] \end{cases}, \tag{1.16}$$

where the matrices A and B are called the *Bogoliubov coefficients*. Moreover,

$$\begin{cases} a_\lambda = \int \mathrm{d}\mu(\kappa) \left[A_{\kappa\lambda} b_\kappa + B_{\kappa\lambda}^* b_\kappa^\dagger \right] \\ b_\kappa = \int \mathrm{d}\mu(\lambda) \left[A_{\kappa\lambda}^* a_\lambda - B_{\kappa\lambda}^* a_\lambda^\dagger \right] \end{cases}. \tag{1.17}$$

Consequently, the vacuum $|0_w\rangle$ will not be annihilated by b_κ, nor will $|0_u\rangle$ be annihilated by a_λ. Furthermore, the w-vacuum expectation value of the number operator N_λ, defined in Eq. 1.13, will not be zero:

$$\begin{aligned} \langle 0_w | N_\lambda | 0_w \rangle &= \langle 0_w | a_\lambda^\dagger a_\lambda | 0_w \rangle \\ &= \langle 0_w | \int \mathrm{d}\mu(\kappa) \int \mathrm{d}\mu(\sigma) \left[A_{\kappa\lambda}^* b_\kappa^\dagger + B_{\kappa\lambda} b_\kappa \right] \left[A_{\sigma\lambda} b_\sigma + B_{\sigma\lambda}^* b_\sigma^\dagger \right] | 0_w \rangle \\ &= \int \mathrm{d}\mu(\kappa) \int \mathrm{d}\mu(\sigma) \langle 0_w | B_{\kappa\lambda} B_{\sigma\lambda}^* b_\kappa b_\sigma^\dagger | 0_w \rangle \\ &= \int \mathrm{d}\mu(\kappa) \int \mathrm{d}\mu(\sigma) \langle 0_w | B_{\kappa\lambda} B_{\sigma\lambda}^* \left[b_\kappa, b_\sigma^\dagger \right] | 0_w \rangle \\ &= \int \mathrm{d}\mu(\kappa) \int \mathrm{d}\mu(\sigma)\, B_{\kappa\lambda} B_{\sigma\lambda}^* \delta(\kappa - \sigma) \\ &= \int \mathrm{d}\mu(\kappa)\, |B_{\kappa\lambda}|^2. \end{aligned} \tag{1.18}$$

In other words, the w-vacuum, although devoid of w-particles, is filled with u-particles. The globally non-stationary character of the spacetime leads to the presence of particles at late times. Note that in this scenario, the particle concept is meaningful at late times only because of the stationarity of the spacetime at late times.

1.3 Quantum effects in Schwarzschild spacetime

The Schwarzschild black hole spacetime discussed in Section 1.1 is a purely static, relativistic spacetime. As long as the black hole's exterior is a vacuum, the black hole does not change in time. However, the picture changes dramatically if quantum theory is added to the mix. Even though, classically, matter cannot escape from a black hole once it has crossed its event horizon, the phenomenon of quantum tunnelling allows matter to leak from the black hole and drain it from its mass, charge, and angular momentum in the process [48]. In this section, we will discuss one of the mechanisms by which particles are created in black hole spacetimes: Hawking radiation.

In the previous section, we constructed QFTCS from the perspective of canonical quantisation. However, in QFTCS, as in regular QFT, multiple perspectives on quantisation coexist. Each is useful in different settings. The point of view of canonical quantisation is particularly well-suited to the discussion of the role of particles in QFTCS. In the context of quantum tunnelling phenomena, the perspective of path integral quantisation is more convenient. Especially the apparatus of Euclidean path integrals and instantons will be extremely useful in our discussions of the Hawking and Schwinger effects. Therefore, before we discuss the Hawking effect, we will first investigate the role of path integrals and instantons in the description of quantum tunnelling phenomena.

1.3.1 Instantons and quantum tunnelling

A good and intuitive definition of instantons can be found in [47], on which the discussion in this section is based (cf. [17] for an older but very influential treatment of instantons):

> Given a quantum system, an instanton is a solution of the equations of motion of the corresponding classical system; however, not for ordinary time, but for the analytically continued classical system in imaginary time. This means that we replace t with $-i\tau$ in the classical equations of motion. Such solutions are alternatively called the solutions of the Euclidean equations of motion.

However, this definition does not explain why instantons are interesting. To get there, consider the Feynman path integral representation of a transition amplitude from an initial state x_i at time t_i to a final state x_f at time t_f for a system evolving according to the quantum Hamiltonian $\hat{H}$ (in the Schrödinger picture):

$$\langle x_f, t_f | e^{-\frac{i}{\hbar}\hat{H}(t_f - t_i)} | x_i, t_i \rangle = \int_{x(t_i)=x_i}^{x(t_f)=x_f} \mathcal{D}x e^{\frac{i}{\hbar}S[x]}, \tag{1.19}$$

where $S[x]$ is the classical action of the path x. It gives a very intuitive understanding of the meaning of the transition amplitude: we integrate over all possible trajectories starting at x_i at time t_i and ending at x_f at time t_f and weight them with a factor $e^{\frac{i}{\hbar}S[x]}$, which depends on the classical action. In the semi-classical limit ($\hbar/S \ll 1$), the dominant contributions to the path integral will come from paths in the vicinity of the classical (on-shell) path, which makes the action stationary. This is because variations of paths for which the action is not (nearly) stationary will cause erratic variations of the exponential $e^{\frac{i}{\hbar}S[x]}$, which tend to cancel each other out.

A key phenomenon that distinguishes quantum mechanics from classical mechanics is the phenomenon of quantum tunnelling. In some quantum-mechanical systems, a particle

can, with a certain non-zero probability, be found in states that are classically prohibited. For example, an alpha particle can tunnel through the potential barrier of the nucleus of an unstable atom, even if it does not have enough kinetic energy to do so classically. If the energy E of the particle is given in terms of its kinetic energy T and potential energy V by

$$E = T + V = \frac{\dot{q}^2}{2} + V(q), \tag{1.20}$$

then for the particle to be in a state with energy $E < V(q)$ it is required that $T = \frac{\dot{q}^2}{2} < 0$. However, negative kinetic energies do not make sense in a classical context, and that means that in the semi-classical limit, there is no classical path available between a classically allowed state and a classically forbidden state to make the action in Eq. 1.19 stationary. However, if we rotate our time coordinate onto the imaginary axis ($t \to -i\tau$)[5], then

$$\left(\frac{\mathrm{d}q}{\mathrm{d}t}\right)^2 \to \left(i\frac{\mathrm{d}q}{\mathrm{d}\tau}\right)^2 = -\left(\frac{\mathrm{d}q}{\mathrm{d}\tau}\right)^2. \tag{1.21}$$

In other words, T becomes negative and we can describe states that are classically unattainable. The signature of our spacetime changes from Lorentzian $(-,+,+,+)$ to Euclidean $(+,+,+,+)$, and we obtain the Euclidean version of the Feynman path integral:

$$\langle x_f, \tau_f | e^{-\frac{\hat{H}}{\hbar}(\tau_f - \tau_i)} | x_i, \tau_i \rangle = \int_{x(\tau_i)=x_i}^{x(\tau_f)=x_f} \mathcal{D}x e^{\frac{-S_E[x]}{\hbar}}, \tag{1.22}$$

where $S_E = -iS$. The imaginary, oscillating exponential of Eq. 1.19 becomes a real, decaying exponential in Eq. 1.22. This exponential decaying behaviour is typical of tunnelling processes such as vacuum decay. Paths that make the Euclidean action S_E stationary are called instanton solutions.

1.3.2 Hawking radiation

The Hawking effect can be derived in the canonical quantisation framework we laid out in Section 1.2 by considering the spherically symmetric gravitational collapse of a ball of matter surrounded by a vacuum. This is the model for which Hawking himself first derived his results [32, 33]. Intuitively, the occurrence of the Hawking effect can be understood as follows. Throughout the collapse, the exterior geometry is unaltered (consistent with Newton's shell theorem generalized to general relativity). However, quantum fields propagating through the interior of the collapsing ball will be dramatically disrupted. If we assume that in the distant past the volume of the ball of matter is very large, such that the matter is very dilute, we can approximate the spacetime as Minkowski spacetime. The spacetime outside the collapsing ball of matter is Schwarzschild spacetime. Consequently, the vacuum in the distant future will not be the same as the vacuum in the distant past. It is precisely this fact that explains the presence of particles in the future spacetime (cf. Section 1.2.3). Importantly, however, the Hawking effect also occurs in eternal black hole spacetimes. This suggests that the Hawking effect does not essentially presuppose gravitational collapse but rather is a feature of the more structural aspects of spacetimes [9].

[5]The conditions under which a field theory in Euclidean space can be reconstructed as a quantum field theory in Lorentzian spacetime were rigorously formulated by Osterwalder and Schrader [44].

The Hawking effect was later derived many times again from multiple points of view, notably from path integrals [27, 30], as a quantum tunnelling effect [48], and using a heat-kernel method [68]. Here, we will give a rough sketch of a derivation by Gibbons and Hawking [27] using the Euclidean action. To start, consider a Euclidean Schwarzschild spacetime with metric

$$\mathrm{d}s^2 = \left(1 - \frac{2M}{r}\right)\mathrm{d}\tau^2 + \left(1 - \frac{2M}{r}\right)^{-1}\mathrm{d}r^2 + r^2\,\mathrm{d}\Omega_2^2\,. \tag{1.23}$$

Next, we zoom in on the black hole horizon by using the coordinate transformation $r = 2M + \lambda\rho$, and expanding the metric to first order around $\lambda = 0$. The result is

$$\mathrm{d}s^2 = \frac{\rho}{2M}\,\mathrm{d}\tau^2 + \frac{2M}{\rho}\,\mathrm{d}\rho^2 + (2M)^2\,\mathrm{d}\Omega_2^2\,. \tag{1.24}$$

Then we define a new radial coordinate x by $\rho = \frac{x^2}{8M}$, and the metric becomes

$$\mathrm{d}s^2 = \left(\frac{x}{4M}\right)^2\mathrm{d}\tau^2 + \mathrm{d}x^2 + (2M)^2\,\mathrm{d}\Omega_2^2\,. \tag{1.25}$$

Now note that the (τ, x) part of this metric is just flat Euclidean space expressed in polar coordinates. The Euclidean time coordinate τ takes on the role of the angular coordinate and has a period of $\Delta\tau = 8\pi M$. If the τ coordinate did not have this period, there would be a conical singularity at the horizon, and the spacetime would not be regular. Thus, the near-horizon limit of Euclidean Schwarzschild space is $E_2 \times S^2$.

Now consider a real scalar field ϕ propagating through this spacetime. Its dynamics are dictated by a Hamiltonian $\hat{H}$, or, equivalently, by an action S. The amplitude for the field to go from a state ϕ_0 at time τ_0 to a state ϕ_1 at time τ_1 is given by $\langle\phi_1, \tau_1|\phi_0, \tau_0\rangle$. This amplitude can be calculated in two different ways: from the Hamiltonian,

$$\langle\phi_1, \tau_1|\phi_0, \tau_0\rangle = \langle\phi_1|e^{-\hat{H}(\tau_1 - \tau_0)}|\phi_0\rangle, \tag{1.26}$$

or from the action,

$$\langle\phi_1, \tau_1|\phi_0, \tau_0\rangle = \int \mathcal{D}\phi e^{-S_E[\phi]}. \tag{1.27}$$

Define $\beta = \tau_1 - \tau_0$, and consider the amplitude for the field to remain in state ϕ_0. Then

$$\langle\phi_0, \tau_0 + \beta|e^{-\beta\hat{H}}|\phi_0, \tau_0\rangle = \mathrm{Tr}\, e^{-\beta\hat{H}} = \int_{\phi(\tau_0)=\phi_0}^{\phi(\tau_0+\beta)=\phi_0} \mathcal{D}\phi e^{-S_E[\phi]}. \tag{1.28}$$

Note that the left-hand side of this expression is the partition function for the canonical ensemble of a field ϕ at finite temperature $T = 1/\beta$ (setting the Boltzmann constant to 1). But the period of the τ coordinate near the horizon was previously found to be $8\pi M$. Consequently, we can identify $\beta = 8\pi M$, and thus

$$T = \frac{1}{8\pi M} \tag{1.29}$$

is to be identified as the temperature of the black hole horizon.[6]

[6]Of course, if one wishes to be rigorous, some more work goes into deriving this relation: one first constructs the Hartle-Hawking vacuum and then shows that it satisfies the Kubo-Martin-Schwinger condition, which implies that Hawking radiation is thermal.

The Hawking effect is not limited to the production of massless scalar particles. In fact, high-mass (low-temperature) Schwarzschild black holes are expected to emit mainly massless non-scalar neutrinos, photons, and gravitons [45], while low-mass (high-temperature) black holes are predicted to also emit massive charged particles such as electrons and muons [46].

Conclusion

In this chapter, we explained how even in a semi-classical treatment, quantum fields can couple to gravity, thereby giving rise to exciting new phenomena, such as Hawking radiation. Along the way, we also introduced the framework of path integral quantisation and the usefulness of instantons in describing quantum tunnelling phenomena. Using instantons, we were able to derive the Hawking effect for Schwarzschild black holes. In Chapters 2 and 4, we will make extensive use of instantons to derive the Schwinger effect around charged black holes, both in asymptotically flat and asymptotically de Sitter spacetimes.

Chapter 2

Schwinger effect in asymptotically flat spacetime

Introduction

The Hawking effect is not exclusive to Schwarzschild black holes but also manifests itself in more general black hole spacetimes, such as the Reissner-Nordström spacetime describing a charged black hole. As discussed in Section 1.3.2, a significant portion of the particles produced around a low-mass black hole are electron-positron pairs. In the case of a small charged black hole, the production of these electron-positron pairs allows for a swift discharge of the black hole due to the presence of the black hole's electric field [26].

However, the Hawking effect is not the only mechanism through which charged black holes discharge. Another mechanism is the so-called *Schwinger effect*: the spontaneous production of oppositely charged particle-antiparticle pairs from the vacuum in the presence of an electric field. For very massive charged black holes, the Schwinger effect will be dominant; for very light charged black holes, the Hawking effect is dominant [26]. In this chapter, we present a calculation, previously performed by [37], of the spatial profile of the production rate of charged particles around a charged black hole in asymptotically flat spacetime. The analysis given here will, in Chapter 4, serve as a blueprint for similar calculations in the significantly more complex context of a Reissner-Nordström black hole placed in a spacetime that is asymptotically de Sitter.

The contents of the present chapter are as follows. In Section 2.1, we introduce, from a classical point of view, the Reissner-Nordström spacetime. Next, in Section 2.2, we give some background on the Schwinger effect and display an (abridged) derivation of the Schwinger production rate in Minkowski spacetime. In Section 2.3, we introduce the worldline formalism, the formalism that we will exploit to calculate the Schwinger rate, and illustrate its use with the help of a toy example. Finally, in Section 2.4, we will apply the worldline formalism to a Reissner-Nordström spacetime with the goal of gaining a better understanding of the spatial profile of the Schwinger rate in this spacetime; in this derivation, instantons will play an essential role.

2.1 Reissner-Nordström black holes in general relativity

We discussed the geometry of the simplest black hole possible, the Schwarzschild black hole, in Section 1.1. A black hole solution to the Einstein field equations that is only slightly more complex is the Reissner-Nordström (RN) black hole, a black hole with mass and charge but without angular momentum. Its exterior is well described by the metric

$$\mathrm{d}s^2 = -f(r)\,\mathrm{d}t^2 + f^{-1}(r)\,\mathrm{d}r^2 + r^2\,\mathrm{d}\Omega_2^2, \tag{2.1}$$

where the blackening factor[1] is given by

$$f(r) = 1 - \frac{2M}{r} + \frac{Q^2}{r^2}, \tag{2.2}$$

and where Q can be interpreted as the black hole's constant electric charge.[2] The charge Q creates an electric field centred at $r = 0$ with electromagnetic tensor F and four-potential A given by

$$F = \mathrm{d}A, \quad A = \frac{Q}{r}\,\mathrm{d}t\,. \tag{2.3}$$

In the chargeless limit ($Q \to 0$), RN black holes become Schwarzschild black holes and, like Schwarzschild black holes, RN spacetimes are asymptotically flat.

Like the Schwarzschild black hole, the RN black hole has a gravitational singularity at $r = 0$. However, unlike the Schwarzschild black hole, the RN black hole has two additional coordinate singularities, determined by the quadratic equation $f(r) = 0$. The solutions are

$$r_\pm = M \pm \sqrt{M^2 - Q^2}. \tag{2.4}$$

Depending on the values of the parameters M and Q, the black hole will have two, one, or no horizons. Let us briefly consider each case (graphically summarized in Figure 2.1).

First, if $M > Q$, the RN black hole has two distinct horizons. The blackening factor is positive for $r > r_+$, negative for $r_- < r < r_+$, and again positive for $r < r_-$. Between the two horizons, r is thus a timelike coordinate. This means that as one crosses the horizon at r_+, one can only keep moving in the direction of r_-. However, once the horizon at r_- is crossed, r becomes spacelike again, and the infalling observer can avoid the singularity at $r = 0$ and move out of the black hole again. The resulting black hole is called a *sub-extremal* RN black hole.

Secondly, if $M = Q$, the two horizon solutions coincide and the event horizon at $r = M$ becomes degenerate. In this case, the RN black hole is called *extremal*. The blackening factor is everywhere positive, which means that the singularity at $r = 0$ is always avoidable. This extremal limit of RN black holes is very interesting from a theoretical point of view, and limits of RN black holes with degenerate horizons will feature prominently in this thesis.

Finally, if $M < Q$, the horizons vanish altogether, and the RN black hole exhibits a *naked singularity*, a singularity that is not hidden behind an event horizon. This type of

[1] The blackening factor is so called because it determines the horizon radii of the black hole and thus the behaviour of light in the spacetime. In dimensionful units it is given by $f(r) = 1 - \frac{2GM}{c^2 r} + \frac{1}{4\pi\varepsilon_0}\frac{GQ^2}{c^4 r^2}$.

[2] The RN black hole can also be given a magnetic charge on top of its electric charge. We will not consider this possibility here.

RN black hole is called *super-extremal*. The blackening factor is again everywhere positive, so the singularity is always avoidable. The existence of naked singularities would spell trouble for the predictability of the universe. Therefore, the *weak cosmic censorship conjecture* (WCCC) bars such naked singularities (first proposed in [50], cf. [66] and [61] for discussions). The extremality condition thus serves as an effective upper bound for RN black holes; RN black holes should always satisfy $M \leq Q$. As we will see in Section 3.3, the WCCC is just one of several conjectures placing bounds on physical parameters on the basis of thought experiments, in which black holes often take the lead role. Visiting the extremal boundaries of black holes can thus be tremendously interesting from a theoretical point of view and might teach us a lot about physics in regimes to which we currently have no experimental access.

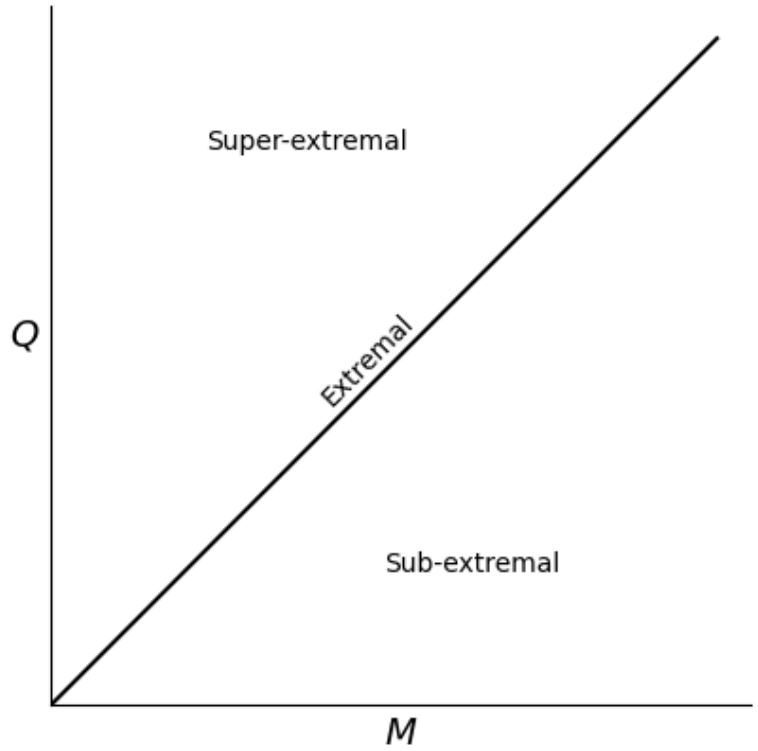

Figure 2.1: Phase space of the RN spacetime. If $Q < M$, there are two horizons, and the black hole is called sub-extremal. If $Q = M$, there is one horizon, and the black hole is called extremal. If $Q > M$, there is no horizon, there is a naked singularity, and the black hole is called super-extremal.

2.2 Schwinger effect in Minkowski spacetime

Not long after the formulation of Dirac's theory of massive spin-1/2 particles [18], which implied the existence of both positive and negative energy electrons (later respectively

called *electrons* and *positrons*), it was suggested by Dirac that this theory predicts the possibility of a scattering event in which an electron and a positron are created and subsequently annihilated in the presence of an electric field [19]. Then, again a bit later, Dirac proposed that the existence of such scattering events (and thus of short-lived particle-antiparticle pairs) in electric fields would lead to the *polarization of the vacuum* [20]. Dirac's proposal led to several calculations of the effects of this vacuum polarization on Maxwell theory [35, 67]. In 1951, almost as an afterthought on an argument about gauge invariance, Schwinger managed to calculate the probability of electron-positron pair creation in a constant electric field, an effect since named the *Schwinger effect* [60].

For the argument, we mainly follow [59]. Consider quantum electrodynamics (QED) with quantum effective action $S_{\text{eff}}[A]$ defined by

$$e^{iS_{\text{eff}}[A]} = \int \mathcal{D}\bar{\psi}\mathcal{D}\psi e^{iS[\psi,\bar{\psi},A]}, \tag{2.5}$$

where the Dirac fields ψ and $\bar{\psi}$ are integrated out of the full action S given by

$$S[\psi,\bar{\psi},A] = \int \mathrm{d}^4x \left(-\frac{1}{4}F_{\mu\nu}F^{\mu\nu} + \bar{\psi}(i\gamma^\mu D_\mu - m)\psi\right) \tag{2.6}$$

where $F_{\mu\nu} = \partial_\mu A_\nu - \partial_\nu A_\mu$, γ^μ are the Dirac matrices, and $D_\mu = \partial_\mu + ieA_\mu$. The quantum effective action (we will drop the 'quantum' qualifier from now on) is an extension of the classical action that incorporates all quantum corrections. Varying the effective action leads to the equations of motion for the vacuum expectation values of the quantum fields involved. The effective Lagrangian $\mathcal{L}_{\text{eff}}$, defined by

$$S_{\text{eff}}[A] = \int \mathrm{d}^4x\, \mathcal{L}_{\text{eff}}(x), \tag{2.7}$$

is called the Euler-Heisenberg Lagrangian $\mathcal{L}_{\text{EH}}$ in the case of a constant electric field (first derived in [35], and again in [60]). When the field is purely electric, it can be calculated to be [60]

$$\mathcal{L}_{\text{EH}} = \frac{1}{2}E^2 - \frac{1}{8\pi^2}\int_0^\infty \frac{\mathrm{d}s}{s^3}e^{is\varepsilon}e^{-sm^2}\left[eEs\cot(eEs) - 1 + \frac{1}{3}(esE)^2\right], \tag{2.8}$$

with poles due to the cotangent for $s = s_n = \frac{n\pi}{eE}$ for $n = 1, 2, 3, \ldots$.

The effective action determines the vacuum-to-vacuum transition amplitude:

$$e^{iS_{\text{eff}}[A]} = \langle 0_{A,\text{out}}|0_{A,\text{in}}\rangle. \tag{2.9}$$

Consequently, the probability for an initial vacuum to end up as a vacuum (the so-called *vacuum persistence probability*) is given by $|e^{iS_{\text{eff}}[A]}|^2$, and thus the probability of vacuum decay is

$$\begin{aligned} P_{\text{dec}} &= 1 - |e^{iS_{\text{eff}}[A]}|^2 \\ &= 1 - e^{i(S_{\text{eff}}[A] - S^*_{\text{eff}}[A])} \\ &= 1 - e^{-2\text{Im}S_{\text{eff}}[A]} \\ &\approx 2\text{Im}S_{\text{eff}}[A], \end{aligned} \tag{2.10}$$

where the last approximation is valid if $\mathrm{Im}S_{\mathrm{eff}}[A] \ll 1$. The imaginary part of the effective action can be computed from Eqs. 2.7 and 2.8 using contour integration and the residue theorem, with the result that [60]

$$\begin{aligned} 2\mathrm{Im}S_{\mathrm{eff}}[A] &= \frac{1}{4\pi}\sum_{n=1}^{\infty}\frac{1}{s_n^2}\exp(-m^2 s_n) \\ &= \frac{\alpha}{2\pi^2}E^2\sum_{n=1}^{\infty}\frac{1}{n^2}\exp\left(\frac{-n\pi m^2}{eE}\right), \end{aligned} \tag{2.11}$$

where α is the fine structure constant. So, the approximation $\mathrm{Im}S_{\mathrm{eff}}[A] \ll 1$ in this case is appropriate for electric fields E and particles with mass m and charge e satisfying $m^2 \gg eE$.

Although Schwinger identified the entirety of P_{dec} as the pair production rate per unit volume, a more careful analysis [16] shows that the pair production rate corresponds only to the leading term of the series in Eq. 2.11:

$$\Gamma = \frac{(eE)^2}{4\pi^3}\exp\left(-\frac{\pi m^2}{eE}\right). \tag{2.12}$$

A more direct calculation of the pair production rate leads to the same conclusion [43]. Eq. 2.11 includes the higher-order contributions to Eq. 2.12. As can be seen from Eq. 2.12, the production rate is higher for stronger electric fields and lower for heavier particles, as expected.

These calculations in Minkowski spacetime show that the Schwinger effect, unlike the Hawking effect, is not an effect that is essentially caused by the interplay of gravity and quantum fields. However, as we will see in the rest of this chapter, and indeed in the rest of this thesis, coupling a charged quantum field to non-trivial gravitational fields leads to altered expressions for the Schwinger pair production rate and new insights into the evolution of charged black holes.

2.3 Worldline formalism

One way to generalize Schwinger's argument and calculation to more general spacetimes is through the so-called *worldline formalism*. It is based on Feynman's path-integral formulation of quantum mechanics [22, 23] and Schwinger's proper time method [60]. Initially inspired by the mathematical apparatus of string perturbation theory, it is also called the *string-inspired formalism* [58]. String techniques can be useful for QFT calculations because string theory reduces to QFT in the limit where the string tension becomes infinite [24, 58]. The goal of the initial use of worldline path integrals was the derivation of rules for the efficient calculation of loop amplitudes in gauge theory [8]. Its use was then expanded by deriving similar rules from first-quantized field theory [62]. Later, an expansion of the formalism to curved spacetimes was achieved [7], which was then applied to the calculation of the effective action for Einstein-Maxwell theory up to one-loop order [6]. Recently, the formalism was used to calculate the effective action and the Schwinger pair production rate in the extremal RN spacetime [37], as we will see in the rest of this chapter.

Here we will illustrate the worldline formalism through a simple example, a real massive scalar field $\phi(x)$ in flat spacetime. The classical action is given by

$$\begin{aligned} S[\phi] &= \int \mathrm{d}^4x \, \frac{1}{2}\left(\partial_\mu\phi\partial^\mu\phi + m^2\phi\right) \\ &= \int \mathrm{d}^4x \, \frac{1}{2}\phi\left(-\Box_t + m^2\right)\phi, \end{aligned} \tag{2.13}$$

where the second equality holds up to boundary terms and where $\Box_t = \eta^{\mu\nu}\partial_\mu\partial_\nu$. Recall that the effective action S_{eff} is given by

$$e^{iS_{\text{eff}}} = \int \mathcal{D}\phi e^{iS[\phi]}. \tag{2.14}$$

Since we are interested in vacuum decay processes, we will work with a Wick-rotated time coordinate $t = -i\tau$. Then the spacetime has Euclidean signature, and the Euclidean effective action S^E_{eff} is given by

$$e^{-S^E_{\text{eff}}} = \int \mathcal{D}\phi e^{-\int \mathrm{d}^4x \, \frac{1}{2}\phi\left(-\Box_\tau + m^2\right)\phi}, \tag{2.15}$$

where $\Box_\tau = \delta^{\mu\nu}\partial_\mu\partial_\nu$. The path integral is Gaussian, which means that

$$\begin{aligned} S^E_{\text{eff}} &= -\ln\left(\left(\det\left(-\Box_\tau + m^2\right)\right)^{-\frac{1}{2}}\right) \\ &= \frac{1}{2}\operatorname{Tr}\ln\left(-\Box_\tau + m^2\right), \end{aligned} \tag{2.16}$$

where we applied the trace-determinant identity in the last line. We then rewrite this expression in the Schwinger proper time representation (which is valid for positive definite operators) and perform the trace in the position basis:

$$\begin{aligned} \frac{1}{2}\operatorname{Tr}\ln\left(-\Box_\tau + m^2\right) &= -\frac{1}{2}\int_0^\infty \frac{\mathrm{d}s}{s}\operatorname{Tr}\left(e^{-s\left(-\Box_\tau + m^2\right)}\right) \\ &= -\frac{1}{2}\int_0^\infty \frac{\mathrm{d}s}{s}\int \mathrm{d}^4x_0 \langle x_0|e^{-s\left(-\Box_\tau + m^2\right)}|x_0\rangle. \end{aligned} \tag{2.17}$$

In the spirit of the worldline formalism, we can interpret $\langle x_0|e^{-s\left(-\Box_\tau + m^2\right)}|x_0\rangle$ as the transition amplitude for a particle moving under the Hamiltonian $H = -\Box_\tau + m^2$ from position x_0 to the same position x_0 over total proper time s. This is precisely the Feynman path integral for a particle that returns to the same point:

$$\langle x_0|e^{-s\left(-\Box_\tau + m^2\right)}|x_0\rangle = \int_{x(T=0)=x_0}^{x(T=s)=x_0} \mathcal{D}x e^{-\int_0^s \mathrm{d}T\left(\frac{1}{4}\dot{x}_\mu\dot{x}^\mu + m^2\right)}, \tag{2.18}$$

where the dot denotes derivation with respect to T. The object

$$S_{\text{wl}}[\dot{x}] = \int_0^s \mathrm{d}T\left(\frac{1}{4}\dot{x}_\mu\dot{x}^\mu + m^2\right) \tag{2.19}$$

will be called the *worldline action*. By rescaling $s = \frac{s'}{m^2}$ and $T = \frac{s'}{m^2}T'$, the worldlines all have proper time 1, and the worldline action can be conveniently recast as

$$S_{\text{wl}}[\dot{x}] = \int_0^1 \mathrm{d}T \left(\frac{m^2}{4s} \dot{x}_\mu \dot{x}^\mu + s \right), \tag{2.20}$$

where we dropped the primes of the rescaling. So, in sum, we find that

$$S^E_{\text{eff}} = -\frac{1}{2} \int_0^\infty \frac{\mathrm{d}s}{s} \int \mathrm{d}^4 x_0 \int_{x(0)=x_0}^{x(1)=x_0} \mathcal{D}x e^{-\int_0^1 \mathrm{d}T \left(\frac{m^2}{4s} \dot{x}_\mu \dot{x}^\mu + s \right)}. \tag{2.21}$$

This formula has a very intuitive conceptual interpretation: the effective action encodes quantum effects arising from the propagation of virtual particles in closed loops. As we will see, extending this formalism to include interactions with background electromagnetic fields allows us to capture photon–photon interactions via the creation of virtual particle–antiparticle pairs — a manifestly non-classical effect.

2.4 Schwinger effect in extremal Reissner-Nordström spacetime

2.4.1 Effective action

The rest of this chapter is devoted to analysing the methods and reproducing the results of [37]. Consider scalar quantum electrodynamics with a complex scalar field $\phi(x)$ coupled to a gauge field $A_\mu(x)$ in a generic spacetime with vanishing Ricci scalar ($R(x) = 0$). The action is given by

$$S[\phi, \phi^*] = \int \mathrm{d}^4 x \sqrt{-g} \frac{1}{2} \phi^* H_A \phi, \tag{2.22}$$

where $H_A = g^{\mu\nu} D_\mu D_\nu - m^2$, $D_\mu = \nabla_\mu + ieA_\mu$, ∇_μ represents the covariant derivative, and $g_{\mu\nu}$ is the spacetime metric. We neglect the dynamics of the gauge field and the background spacetime. In other words, we study a semi-classical approximation and do not consider backreactions of the field on the metric or gauge field. Since A and g are fixed, the Maxwell and Einstein-Hilbert action terms would just add a constant phase to the total action. However, to calculate the Schwinger rate, we only need to calculate a vacuum expectation value (cf. Eq. 2.9), which is not affected by the phase. Consequently, these action terms can be safely omitted here.

We again work in Euclidean time. As before, since the action 2.22 is quadratic in ϕ, the Euclidean path integral over ϕ and ϕ^* can be written as a functional determinant:

$$\int \mathcal{D}\phi^* \mathcal{D}\phi e^{-S_E} = (\det H_A)^{-\frac{1}{2}}. \tag{2.23}$$

The Euclidean effective action is given by

$$\begin{aligned} S_{\text{eff}}^{E} &= \frac{1}{2}\ln\left(\det H_A\right) \\ &= \frac{1}{2}\operatorname{Tr}\ln H_A \\ &= -\frac{1}{2}\int_0^\infty \frac{\mathrm{d}s}{s}\operatorname{Tr}\left(e^{-sH_A}\right) \\ &= -\frac{1}{2}\int_0^\infty \frac{\mathrm{d}s}{s}\int \mathrm{d}^4x_0\,\sqrt{-g}\langle x_0|e^{-sH_A}|x_0\rangle. \end{aligned} \tag{2.24}$$

Again interpreting the kernel as a path integral, we find

$$\langle x_0|e^{-sH_A}|x_0\rangle = \int_{x(T=0)=x_0}^{x(T=s)=x_0} \mathcal{D}x e^{-\int_0^s \mathrm{d}T\left[\frac{1}{4}\dot{x}_\mu\dot{x}^\mu + eA_\mu\dot{x}^\mu + m^2\right]}. \tag{2.25}$$

Rescaling the same way as before (cf. Eq. 2.20), we find an expression for the worldline action,

$$S_{\text{wl}}\left[s,x\right] = \int_0^1 \mathrm{d}T\left(\frac{m^2}{4s}\dot{x}_\mu\dot{x}^\mu + eA_\mu\dot{x}^\mu + s\right), \tag{2.26}$$

and for the Euclidean effective action,

$$S_{\text{eff}}^{E} = -\frac{1}{2}\int_0^\infty \frac{\mathrm{d}s}{s}\int \mathrm{d}^4x_0\,\sqrt{-g}\int_{x(0)=x_0}^{x(1)=x_0} \mathcal{D}x e^{-\int_0^1 \mathrm{d}T\left(\frac{m^2}{4s}\dot{x}_\mu\dot{x}^\mu + eA_\mu\dot{x}^\mu + s\right)}. \tag{2.27}$$

As is manifest from Eq. 2.27, the contribution of paths with large worldline action will be exponentially suppressed. Consequently, we can approximate the path integral by expanding the worldline action around the stationary point $(\bar{s},\bar{x})$ corresponding to the classical path starting and ending at $x = x_0$. This we will do in the next section. However, we must account for the fact that the global Schwinger pair production rate will be infinite. Moreover, we are interested in the radial profile of the Schwinger rate, and thus we want to have at our disposal a more local description of the effective action. To this end, we define the *local* effective action $w(x_0)$ by

$$S_{\text{eff}}^{E} = \int \mathrm{d}^4x_0\,\sqrt{-g}w(x_0). \tag{2.28}$$

Explicitly,

$$\begin{aligned} w(x_0) &= -\frac{1}{2}\int_0^\infty \frac{\mathrm{d}s}{s}\int_{x(T=0)=x_0}^{x(T=1)=x_0} \mathcal{D}x e^{-S_{\text{wl}}[s,x]} \\ &\approx \frac{1}{2}\mathcal{A}(\bar{x})e^{-S_{\text{wl}}[\bar{s},\bar{x}]}. \end{aligned} \tag{2.29}$$

Here, the *one-loop determinant* $\mathcal{A}$ encodes the one-loop quantum fluctuations around the classical path. The local Schwinger rate will then be given by

$$\Gamma(x_0) = 2\mathrm{Im}w(x_0) = |\mathcal{A}(\bar{x})|e^{-S_{\text{wl}}[\bar{s},\bar{x}]}. \tag{2.30}$$

2.4.2 Worldline instantons

The expansion of the worldline action up to second order can be found in [37]. Imposing vanishing first variations, we find the stationary point

$$\begin{cases} \bar{s} = \frac{m}{2}\sqrt{\dot{\bar{x}}_\mu \dot{\bar{x}}^\mu} \\ \left(\frac{m^2}{2\bar{s}}\frac{D^2\bar{x}_\mu}{\mathrm{d}T^2} - eF_{\mu\nu}\frac{D}{\mathrm{d}T}\bar{x}^\nu\right) = 0 \end{cases}, \tag{2.31}$$

where $F_{\mu\nu} = \partial_\mu A_\nu - \partial_\nu A_\mu$. We will call these solutions the *worldline instantons*. Note that $\bar{s}$ can be interpreted as a rescaled total proper time along the worldline, while the second equation can be seen as the geodesic equation of a charged particle moving through an electric field in a curved spacetime, where $\dot{\bar{x}}^\mu \coloneqq \frac{D\bar{x}^\mu}{\mathrm{d}T}$ is the particle velocity along the worldline. Contracting the geodesic equation with the particle velocity and using the fact that F is an antisymmetric (0,2)-tensor, we find that

$$\frac{D}{\mathrm{d}T}\left(\dot{\bar{x}}_\mu \dot{\bar{x}}^\mu\right) = 0, \tag{2.32}$$

and thus

$$g_{\mu\nu}\dot{\bar{x}}^\mu \dot{\bar{x}}^\nu = a^2 = \text{const.}, \tag{2.33}$$

where a can be viewed as a normalisation constant. Consequently, $\bar{s} = ma/2$.

We now make some simplifying assumptions. First, we choose the gauge field to be static: $A(r) = A_0(r)\,\mathrm{d}\tau$, so that $F(r) = -\frac{A_0(r)}{r}\,\mathrm{d}r \wedge \mathrm{d}\tau$. Secondly, we assume the spacetime to be spherically symmetric with coordinates (τ, r, θ, ϕ). Thirdly, we assume that the particles have no angular momentum. This assumption is justified since adding angular momentum would increase the worldline action, suppressing the contribution to the path integral. Dropping the overbars, we then find the following equations from Eq. 2.31:

$$\begin{cases} \frac{m}{a}\frac{D^2\tau}{\mathrm{d}T^2} = eF^0{}_1\frac{Dr}{\mathrm{d}T} \\ \frac{m}{a}\frac{D^2r}{\mathrm{d}T^2} = -eF^1{}_0\frac{D\tau}{\mathrm{d}T} \end{cases}. \tag{2.34}$$

From the first of these, we retrieve a conserved quantity ω that looks like the energy of the instanton particle:

$$\omega = \frac{m}{a}g_{00}\dot{\tau} + eA_0, \tag{2.35}$$

and combining this with 2.33, we find

$$\dot{r} = \pm a\sqrt{g_{11}^{-1}\left[1 - \frac{(eA_0 - \omega)^2}{m^2 g_{00}}\right]}. \tag{2.36}$$

We continue calculating the worldline instanton action

$$S_{\mathrm{wl}}\left[\bar{s}, \bar{x}\right] = \int_0^1 \mathrm{d}T\left(\frac{m^2}{4\bar{s}}\dot{\bar{x}}_\mu\dot{\bar{x}}^\mu + eA_\mu\dot{\bar{x}}^\mu + \bar{s}\right). \tag{2.37}$$

Using Eq. 2.33 and the expression for $\bar{s}$, the first and last terms each contribute $ma/2$, for a total of ma. The second term contributes $e\int_0^1 \mathrm{d}T\, A_0\dot{\tau}$. At this point, we need to specify our spacetime to proceed.

2.4.3 Extremal Reissner-Nordström instantons

We specialise to RN spacetime. More specifically, we restrict our investigations to extremal RN black holes (cf. Section 2.1), since these are most interesting from the point of view of fundamental physics. For extremal RN black holes, $M = Q$, so the Euclidean metric and the gauge field are given by

$$\mathrm{d}s^2 = f(r)\,\mathrm{d}\tau^2 + \frac{\mathrm{d}r^2}{f(r)} + r^2\,\mathrm{d}\Omega_2^2, \quad A = \frac{Q}{r}\,\mathrm{d}\tau, \tag{2.38}$$

where

$$f(r) = \left(1 - \frac{Q}{r}\right)^2. \tag{2.39}$$

The degenerate horizon is located at $r = Q$. The instanton equation of motion, Eq. 2.36, specialised to this spacetime is

$$\dot{r} = \pm a\sqrt{\left(1 - \frac{Q}{r}\right)^2 - \frac{e^2}{m^2}\left(\frac{Q}{r} - \frac{\omega}{e}\right)^2}. \tag{2.40}$$

We define some new symbols to simplify things. We introduce a new radial coordinate $\rho = Q/r$, which maps the exterior of the RN black hole to $\rho = (0, 1)$, with the horizon at $\rho = 1$; the charge-to-mass ratio of the instanton particle is $z = e/m$; and the particle's energy is rescaled as $\rho_0 = \omega/e$. The previous equation then simplifies to

$$\dot{\rho} = \mp\frac{a}{Q}\rho^2\sqrt{h(\rho)}, \tag{2.41}$$

where

$$h(\rho) = (1 - \rho)^2 - z^2(\rho - \rho_0)^2 \tag{2.42}$$

acts as an effective potential in the radial direction. The zeros of h can be calculated as $\rho_{1,2} = \frac{z\rho_0 \pm 1}{z \pm 1}$. The radial equation Eq. 2.41 can be solved analytically [37], but the analytic solution is not of any real interest here. From Eq. 2.35 we find

$$\dot{\tau} = \frac{za(\rho_0 - \rho)}{f(\rho)}. \tag{2.43}$$

Combining this with Eq. 2.41, we get

$$\frac{\mathrm{d}\tau}{\mathrm{d}\rho} = \frac{\dot{\tau}}{\dot{\rho}} = \mp Qz\frac{\rho_0 - \rho}{\rho^2 f(\rho)\sqrt{h(\rho)}}. \tag{2.44}$$

Two things are worth noting here. First, because of the asymptotical flatness of the RN spacetime, the charge and mass of the black hole are well defined at radial infinity. The charge and mass of emitted particles that escape to radial infinity are therefore subtracted from those of the black hole. (It will be a major challenge in chapter 4 to determine what happens to the charge and mass of a black hole in an asymptotically de Sitter spacetime.) The prohibition of naked singularities implies the black hole extremality bound ($Q \leq M$). Consequently, only super-extremal particles, for which $q > m$, can be emitted from the RN black hole. So when computing the Schwinger production rate, we should only include particles for which $z = e/m > 1$. Secondly, since the only paths

that contribute to the Euclidean effective action 2.27 are those with the same starting and ending points, the time and radial coordinates should both admit turning points. In other words, the particles have to go around in loops in both the radial and Euclidean time directions. For there to be loops, the black hole exterior must allow for at least two turning points, i.e. two radii where $\dot{\rho}$ vanishes. By demanding that the roots of $h(\rho)$ be real, distinct, and lie between radial infinity and the horizon (in the interval $(0, 1)$), we can find the constraint $\rho_0 \in (\frac{1}{z}, 1)$.[3] The looping instanton path is sketched in Figure 2.2.

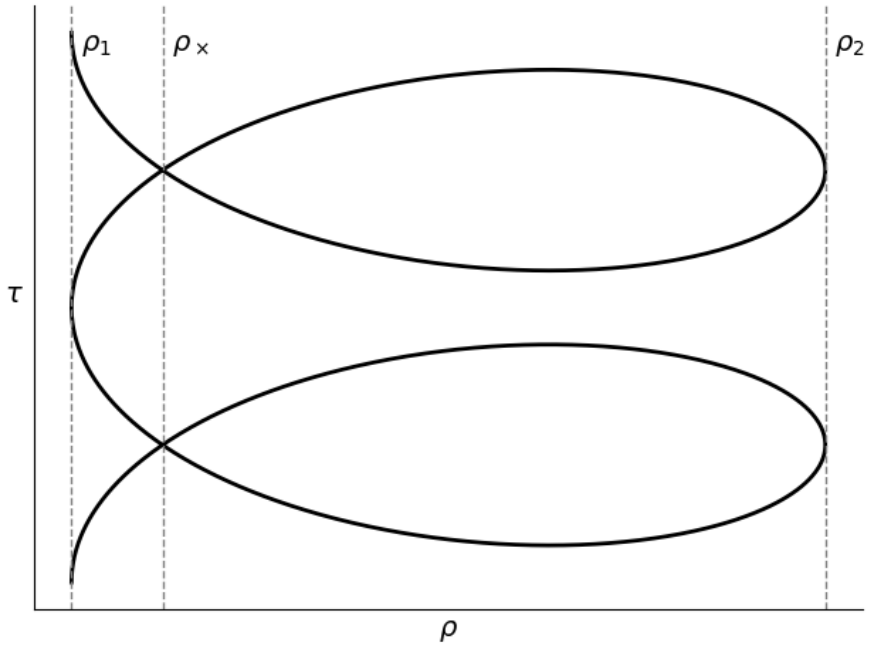

Figure 2.2: Sketch of the looping instanton path. The parts of the curve between $\rho_\times$ and ρ_2 contribute to the instanton action. Figure reconstructed from [37].

We denote the starting and ending point of the looping path by $\rho(T = 0) = \rho(T = 1) = \rho_\times$ and $\tau(T = 0) = \tau(T = 1) = 0$. The instanton paths are fully determined by a and $\rho_\times$, which can be found by demanding

$$\begin{cases} \rho(T=0) = \rho(T=1) = \rho_\times \\ \rho(T=\frac{1}{2}) = \rho_2 \\ \tau(T=0) = \tau(T=\frac{1}{2}) = 0 \end{cases} . \tag{2.45}$$

Having specialized the worldline path to extremal RN spacetime, we can now continue our calculation of the second term in the worldline instanton action:

$$\begin{aligned} S_A &= e \int_0^1 \mathrm{d}T \, A_0 \dot{\tau} \\ &= e \oint_\gamma \mathrm{d}\rho \, A_0 \frac{\mathrm{d}\tau}{\mathrm{d}\rho} \\ &= Qm \frac{z^2}{\sqrt{z^2-1}} \times 2I, \end{aligned} \tag{2.46}$$

[3] In [37], the constraint is mistakenly given as $\rho_0 \in (0, 1)$.

where γ represents the closed loop over which we integrate and

$$I = \int_{\rho_\times}^{\rho_2} F(\rho)\,\mathrm{d}\rho = \int_{\rho_\times}^{\rho_2} \frac{(\rho_0-\rho)\,\mathrm{d}\rho}{\rho(1-\rho^2)\sqrt{(\rho_2-\rho)(\rho-\rho_1)}}. \tag{2.47}$$

In general, I must be computed numerically. The algorithm to do so is the following. First, fix a value for z. Next, consider a range of ρ_0, constrained by z. The parameter ρ_0, which we previously related to the energy of the produced particles, essentially determines where the particle will be created. Then, for each ρ_0, demand that

$$\mp\frac{1}{Qz}\int_{\rho_\times}^{\rho_2}\mathrm{d}\rho\,\frac{\mathrm{d}\tau}{\mathrm{d}\rho} = \int_{\rho_\times}^{\rho_2}\mathrm{d}\rho\,\frac{\rho_0-\rho}{\rho^2 f(\rho)\sqrt{h(\rho)}} = 0. \tag{2.48}$$

This condition expresses that the total change of the Euclidean time τ over half an instanton loop must be zero. From it, determine $\rho_\times$. Once a value for $\rho_\times$ is found, compute I and determine a/Q by integrating Eq. 2.41:

$$\frac{a}{Q}\int_0^{1/2}\mathrm{d}T = \int_{\rho_\times}^{\rho_2}\mathrm{d}\rho\,\frac{1}{\rho^2\sqrt{h(\rho)}}. \tag{2.49}$$

Finally, compute

$$\frac{1}{Qm}S_{\mathrm{wl}}[\bar{s},\bar{x}] = \frac{a}{Q} + \frac{z^2}{\sqrt{z^2-1}}\times 2I, \tag{2.50}$$

and to each $\rho_\times$ associate a radial distance from the outer horizon at ρ_+:

$$\Delta\rho = \rho_+ - \rho_\times = 1-\rho_\times. \tag{2.51}$$

With this algorithm, we were able to reproduce the results of [37]. A plot of the radial profile of the instanton action for some values of z is given in Fig. 2.3. As far as the exponential term of the Schwinger rate (cf. Eq. 2.12) is concerned, the production of particles with large charge-to-mass ratio z close to the black hole event horizon is preferred. This implies that a swift discharge and thus a swift evolution away from extremality are preferred in RN spacetime.

It is also possible to obtain an analytic solution of the instanton action in the near-horizon limit, where the geometry is $\mathrm{AdS}_2\times\mathrm{S}^2$. This limit corresponds to taking the parameter $\rho_0 \to 1$, since then the two turning points $\rho_{1,2} = \frac{z\rho_0\pm 1}{z\pm 1} \to 1$ tend to the horizon. Moreover, we can approximate $\rho_\times$ by ρ_1. So in the near-horizon limit, we find the following approximation:

$$I \approx \int_{\rho_1}^{\rho_2} F(\rho)\,\mathrm{d}\rho = \int_{\rho_1}^{\rho_2} \frac{(\rho_0-\rho)\,\mathrm{d}\rho}{\rho(1-\rho^2)\sqrt{(\rho_2-\rho)(\rho-\rho_1)}}. \tag{2.52}$$

Using an appropriate contour and the residue theorem, it can be calculated to be

$$2I = 2\pi\left[\frac{\rho_0}{\sqrt{\rho_1\rho_2}} + \frac{\rho_0(2\rho_1\rho_2-3\rho_1-3\rho_2+4)-(2-\rho_1-\rho_2)}{2[(1-\rho_1)(1-\rho_2)]^{\frac{3}{2}}}\right] \tag{2.53}$$

This results in

$$\frac{1}{Qm}S_{\mathrm{wl}}\left[\bar{s},\bar{x}\right] = 2\pi\left[\frac{z^2\rho_0-1}{\left(z^2\rho_0^2-1\right)^{3/2}} + z - \frac{z^2\rho_0}{\sqrt{z^2\rho_0^2-1}}\right]. \tag{2.54}$$

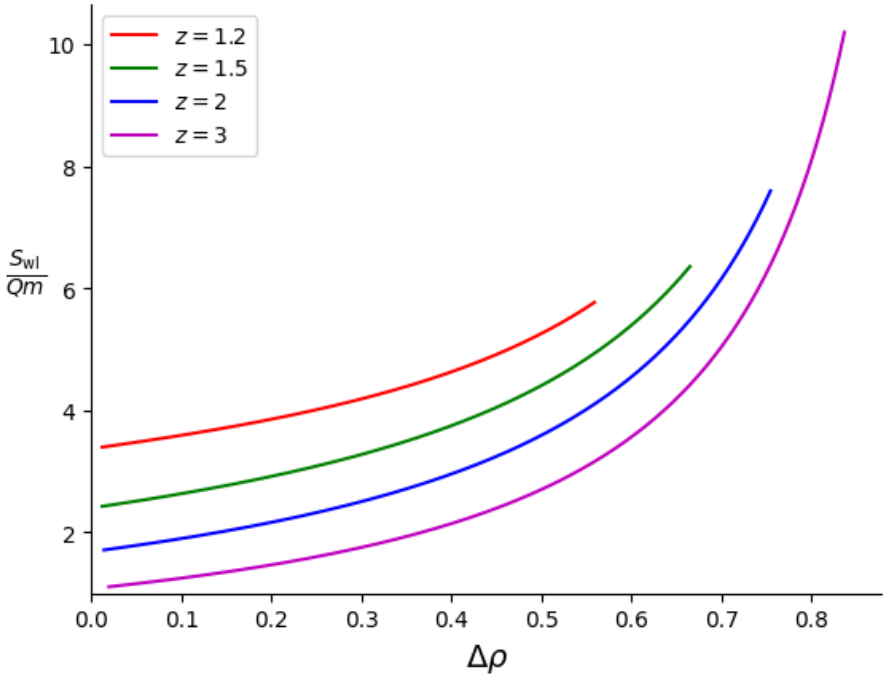

Figure 2.3: Numerical results of the radial profile of the worldline instanton action for some values of z. Note that the curves become shorter for decreasing z. This is due to the fact that for lower z, there are fewer available particle energies $\rho_0 \in (\frac{1}{z}, 1)$, which limits the $\rho_\times$ at which particles can spawn.

A comparison of the numerical result and the analytical approximation can be found in Fig. 2.4. The results converge in the near-horizon limit, as expected.

As a final check, substituting $\rho_{1,2} = \frac{z\rho_0 \pm 1}{z \pm 1}$ and taking $\rho_0 \to 1$ in Eq. 2.54, we find that

$$S_{\text{wl}}\left[\bar{s}, \bar{x}\right] = ma + S_A = 2\pi Qm(z - \sqrt{z^2 - 1}), \tag{2.55}$$

which is the correct expression for the worldline instanton action in $\text{AdS}_2 \times \text{S}^2$ (cf. [57]).

Conclusion

In this chapter, we managed to successfully reproduce the radial profile of the worldline instanton action (and consequently of the Schwinger effect) in asymptotically flat extremal RN spacetime with the help of a numerical solver. The analysis could be extended to include a calculation of the one-loop determinant $\mathcal{A}$, as is done in [37]. However, doing so does not radically alter our conclusions, since the dominant radial dependence of the Schwinger effect is in the exponential factor. Although useful, an explicit calculation of $\mathcal{A}$ is therefore not strictly necessary for our purposes, a sentiment shared by [1]. In Chapter 4, we will attempt to extend the worldline instanton treatment we just presented to RN black holes in asymptotically de Sitter spacetimes. However, before doing so, we will take a closer look at the geometry and semi-classical evolution of such black holes.

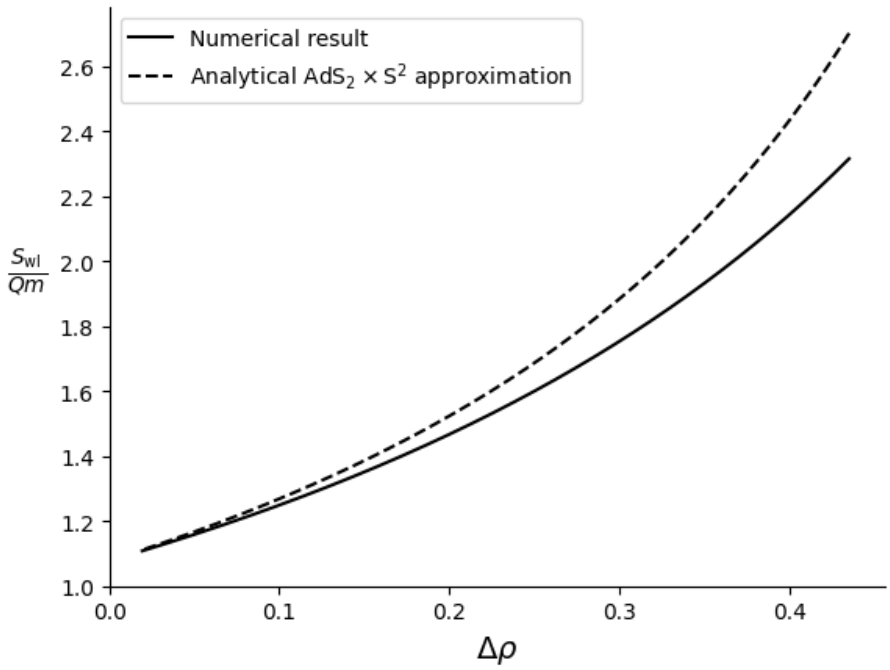

Figure 2.4: Comparison of the numerical result and the analytical $AdS_2 \times S^2$ approximation of the radial profile of the worldline instanton action for $z = 3$. Excellent correspondence is found in the near-horizon limit $\Delta\rho \to 0$.

Chapter 3

Reissner-Nordström-de Sitter spacetime

Introduction

Compared to Minkowski or even anti-de Sitter, de Sitter spacetime is significantly more complex. The main reason for this is the presence of a cosmological horizon. Unsurprisingly, this means that the analysis of an RN black hole in an asymptotically de Sitter spacetime is also markedly more difficult than that of an RN black hole in flat space. Most strikingly, whereas RN-flat black holes can, theoretically, grow as large as they want, the mass and charge of RN black holes in de Sitter have upper bounds. This gives rise to an extremely interesting shape of the black hole's phase space and leads to fascinating questions about the evolution of this object due to its interactions with quantum fields. In particular, if very light charged particles exist, the evolution of charged Nariai black holes under the influence of the Schwinger effect can lead to pathological spacetimes exhibiting crunching behaviour. This has led the authors of [40, 41] to postulate a lower bound on the mass of charged particles, a claim that has not gone unnoticed (or, for that matter, uncriticized) in the literature.

In Chapter 4, we will try to better understand the results of [40] using the machinery we set up in Chapter 2. Before we do so, we introduce the Reissner-Nordström-de Sitter spacetime in the present chapter. It will be structured as follows. In Section 3.1, we will first give a general characterisation of the structure and thermodynamics of de Sitter spacetime, and of its status as a model of our universe. In Section 3.2, we then fill de Sitter space with an RN black hole and investigate its geometry, phase space, and semi-classical evolution, which will lead us to the pathological behaviour mentioned earlier. In Section 3.3, we discuss [40]'s proposal, the so-called *Festina Lente* bound, to prevent this pathological behaviour. We also place it in the larger context of the swampland programme and the search for a theory of quantum gravity.

3.1 de Sitter spacetime

For our discussion of de Sitter spacetime, we will mainly draw on the review article [5]. An important feature of all spacetimes is the number of symmetries they possess. Spacetimes that are more symmetric are typically easier to handle computationally. In general, a

four-dimensional spacetime that is maximally symmetric is characterised by the fact that its Riemann tensor can be written as

$$R_{cdab} = \frac{R}{12}\left(g_{ca}g_{db} - g_{cb}g_{da}\right), \tag{3.1}$$

from which it can be deduced that the Ricci scalar R is a constant throughout the spacetime [34]. Given this condition, it can be seen that there are only three families of maximally symmetric spacetimes, classified by the sign of R. If $R = 0$, the spacetime is Minkowski, if $R < 0$, the spacetime is anti-de Sitter (AdS), and if $R > 0$, the spacetime is called de Sitter (dS). So, dS spacetime is the maximally symmetric spacetime with positive curvature. By tracing the Einstein field equations,

$$R_{ab} - \frac{1}{2}Rg_{ab} + \Lambda g_{ab} = 0, \tag{3.2}$$

it is found that $R = 4\Lambda$. Defining $l^2 = 3/\Lambda$, dS geometry can be described by the induced metric on a four-dimensional hyperboloid

$$-x_0^2 + \sum_{i=1}^{4} x_i^2 = l^2 \tag{3.3}$$

embedded in a five-dimensional Minkowski spacetime:

$$\mathrm{d}s^2 = -\,\mathrm{d}x_0^2 + \sum_{i=1}^{4} \mathrm{d}x_i^2\,. \tag{3.4}$$

Various coordinate patches that satisfy the embedding condition exist, each covering part or the whole of the spacetime manifold, and each useful in different situations. *Global coordinates* cover the maximal extension of the spacetime and are given by

$$\mathrm{d}s^2 = -\,\mathrm{d}T^2 + l^2\cosh^2\frac{T}{l}\left(\mathrm{d}\chi^2 + \sin^2\chi\,\mathrm{d}\Omega_2^2\right). \tag{3.5}$$

Due to the behaviour of the hyperbolic cosine, slices of constant T are 3-spheres that shrink in size for $T \in (-\infty, 0)$ and grow for $T \in (0, \infty)$. The minimal radius l is reached at $T = 0$. Another coordinate system is the so-called *static patch*, given by

$$\mathrm{d}s^2 = -\left(1 - \frac{r^2}{l^2}\right)\mathrm{d}t^2 + \left(1 - \frac{r^2}{l^2}\right)^{-1}\mathrm{d}r^2 + r^2\,\mathrm{d}\Omega_2^2\,. \tag{3.6}$$

The static patch does not describe the entire spacetime, but is valid only for $r \in [0, l)$, which corresponds to the region of space that is causally accessible to an observer positioned at $r = 0$.

Note from the global coordinates that there is no global timelike Killing vector. However, ∂_t is a timelike Killing vector in the static patch. At $r = l$, the norm of this vector becomes null, and for $r > l$ it becomes spacelike, which means that $r = l$ functions as a cosmological event horizon. The situation is quite similar to that of Schwarzschild spacetime: Schwarzschild coordinates (cf. Eq. 1.1) give a good description of the geometry outside the black hole event horizon, allowing for a timelike Killing vector outside the

horizon. To describe the Schwarzschild geometry globally, one needs to transform to, for example, Kruskal-Szekeres coordinates, in which it becomes apparent that there is no global timelike Killing vector. However, there is an important difference between the situation in Schwarzschild and dS. While in Schwarzschild spacetime the position of the event horizon is the same for all observers, the position of the cosmological event horizon in dS is different for all observers. In other words, while Schwarzschild spacetime in a very real sense has a centre, dS has as many centres as there are observers. For each observer, there is a 'point of no return' defined by the cosmological horizon. Information cannot be retrieved from it once it has crossed it.

In Section 1.3.2, we found that we could associate a temperature $T_S = (8\pi M)^{-1}$ with a Schwarzschild black hole. Going through the exact same steps as before, we can associate a temperature to the dS cosmological horizon, as was first suggested in [28]:

$$T_{dS} = (2\pi l)^{-1}. \tag{3.7}$$

As in the case of Schwarzschild spacetime, an observer in dS is predicted to detect a steady flux of particles at this temperature. In the case of Schwarzschild, we can interpret this stream of matter as depleting the black hole of its mass and thus causing it to evaporate. However, in the case of dS, the matter remains part of the dS universe, and it is therefore not entirely clear what the effect of the thermal radiation on the size of the cosmological horizon will be.

In dS, space expands at an increasing rate. There is good reason to believe that our own universe is also expanding at an accelerating rate and thus might be well approximated on cosmological scales as dS [51, 56]. However, two recent discoveries call into question this simplified view of the universe. First, the value of the Hubble constant (the relative rate of expansion of the universe) depends on whether it is measured directly from the redshift of astrophysical objects in the sky or calculated from quantities related to the early universe. This discrepancy is called the *Hubble tension* (cf. [64] for a review). Secondly, the latest results of measurements by the Dark Energy Spectroscopic Instrument (DESI) suggest that the cosmological constant might be dynamical [3]. Nevertheless, gaining a good grasp of physics in dS has lost none of its importance in establishing an understanding of expanding universes.

3.2 Reissner-Nordström-de Sitter spacetime

3.2.1 Classical geometry and energy-momentum

Consider the Einstein-Maxwell-de Sitter action

$$S = \int \mathrm{d}^4x \sqrt{-g} \left[\frac{1}{16\pi} (R - 2\Lambda) - \frac{1}{4} F_{\mu\nu} F^{\mu\nu} \right], \tag{3.8}$$

where R is the Ricci scalar, Λ is a positive cosmological constant, and $F = \mathrm{d}A$ is the electromagnetic field strength tensor for a gauge field A. By varying this action with respect to the gauge field, one finds the equation of motion for F:

$$\nabla_\mu F^{\mu a} = 0. \tag{3.9}$$

By varying with respect to the metric, one recovers the Einstein field equations

$$R_{ab} - \frac{1}{2}Rg_{ab} + \Lambda g_{ab} = 8\pi T_{ab}, \tag{3.10}$$

with energy-momentum tensor

$$T_{ab} = F_{a\mu}F_b{}^{\mu} - \frac{1}{4}g_{ab}F_{\mu\nu}F^{\mu\nu}. \tag{3.11}$$

Tracing the Einstein field equations, we find that $R = 4\Lambda$.

These equations are satisfied by the Reissner-Nordström-de Sitter (RNdS) spacetime, with metric and gauge field

$$\mathrm{d}s^2 = -f(r)\,\mathrm{d}t^2 + \frac{\mathrm{d}r^2}{f(r)} + r^2\,\mathrm{d}\Omega_2^2, \quad A = \frac{Q}{r}\,\mathrm{d}t, \tag{3.12}$$

where the blackening factor is given by

$$f(r) = 1 - \frac{2M}{r} + \frac{Q^2}{r^2} - \frac{r^2}{l^2}. \tag{3.13}$$

We identify M and Q as, respectively, the mass and charge of the black hole. The horizons of the RNdS spacetime solve the equation $f(r) = 0$. Explicitly, they satisfy

$$\frac{r^4}{l^2} - r^2 + 2Mr - Q^2 = 0. \tag{3.14}$$

Being a quartic polynomial equation, it will generically have four roots (with rather lengthy expressions, which can be found in [38]). However, one root always turns out to be negative and is therefore considered unphysical. The other three correspond to an inner, outer and cosmological horizon, with radii respectively $r_- < r_+ < r_c$. Note that we are working in static patch coordinates, suitable for observers between the outer black hole horizon and the cosmological horizon. Only the outer and cosmological horizons are observable to an observer outside of the black hole.

3.2.2 Phase space

The black hole has a phase diagram in the parameters M, Q and l. To avoid naked singularities, we must exclude configurations for which the horizons disappear. These configurations make the discriminant D_4 of the quartic in Eq. 3.14 negative. The boundaries between the forbidden ($D_4 < 0$) and allowed ($D_4 > 0$) regions of the phase space are determined by the condition $D_4 = 0$. In general, the discriminant of a depressed quartic polynomial $ax^4 + cx^2 + dx + e$ is

$$D_4 = 256a^3e^3 - 128a^2c^2e^2 + 144a^2cd^2e - 27a^2d^4 + 16ac^2e - 4ac^3d^2. \tag{3.15}$$

Setting this to zero results in the equation

$$-16\frac{Q^6}{l^6} - 8\frac{Q^4}{l^4} + 36\frac{M^2Q^2}{l^4} - 27\frac{M^4}{l^4} - \frac{Q^2}{l^2} + \frac{M^2}{l^2} = 0. \tag{3.16}$$

The resulting phase diagram, with the boundaries determined by Eq. 3.16, is given in Figure 3.1. For obvious reasons, it is called the shark fin diagram. If $D_4 = 0$, two or three RNdS horizons are degenerate. The upper branch in the phase diagram corresponds to configurations in which the inner and outer horizons coincide ($r_- = r_+$). These configurations are called extremal RNdS black holes. The near-horizon limit for extremal black holes is $AdS_2 \times S^2$ [10]. The lower branch corresponds to the coincidence of the outer and cosmological horizons ($r_+ = r_c$). These configurations are called Nariai RNdS black holes, in analogy to Schwarzschild-de Sitter black holes for which the black hole and cosmological horizons coincide [42]. The near-horizon limit for Nariai black holes is $dS_2 \times S^2$ [10]. Where both branches meet, all three horizons coincide ($r_- = r_+ = r_c$). This configuration is called the ultra-cold black hole, so called because its Hawking temperature is zero [57]. In a sense, it represents the largest possible RNdS black hole. Near the horizon, the geometry of the ultra-cold black hole is approximately $Mink_2 \times S^2$ [10].

Note that the extremal boundary is slightly off-diagonal; it does not coincide with the line $Q = M$. In contrast to the extremal RN spacetime we discussed in Section 2.1, the relation between M and Q is more involved for the extremal RNdS spacetime (cf. Section 4.2). However, the line $Q = M$ is still of interest: it represents the configuration for which the black hole horizon at r_+ and the cosmological horizon at r_c are in thermal equilibrium ($T_+ = T_c$) [57].

3.2.3 Semi-classical evolution

We now analyse the argument given in [40], which leads to the Festina Lente bound. If, following the WCCC (cf. Section 2.1), naked singularities are to be prohibited, the path traced through phase space by evaporating black holes should not leave the interior of the shark fin. It is therefore interesting to investigate how RNdS black holes evolve under the Schwinger and Hawking effects. To get an intuitive understanding, just consider the Schwinger effect in flat spacetime (cf. Section 2.2). The pair production rate

$$\Gamma \propto \exp\left(-\frac{\pi m^2}{qE}\right) \tag{3.17}$$

is highly dependent on the ratio m^2/qE. This suggests that we should distinguish between two regimes determined by the mass and charge of the emitted particles. The first is the quasi-static regime $m^2 \gg qE$, in which the Schwinger rate is exponentially suppressed and the RNdS black hole evolves slowly. The other regime is the adiabatic regime $m^2 \ll qE$, in which the Schwinger rate is exponentially amplified and the RNdS black hole evolves on short timescales. In what follows, we will fix $l = 1$, without loss of generality (although it is possible to let l be dynamical, cf. [38]).

Quasi-static regime ($m^2 \gg qE$)

These calculations were first performed in [40] and were reproduced in [38]. In the regime where the Schwinger effect is exponentially suppressed, we can model the evolution of the RNdS black hole by adding a small perturbation to the metric and the energy-momentum tensor:

$$\tilde{g}_{ab} = g_{ab} + \epsilon\delta g_{ab}, \quad \tilde{F}_{ab} = F_{ab} + \epsilon\delta F_{ab}. \tag{3.18}$$

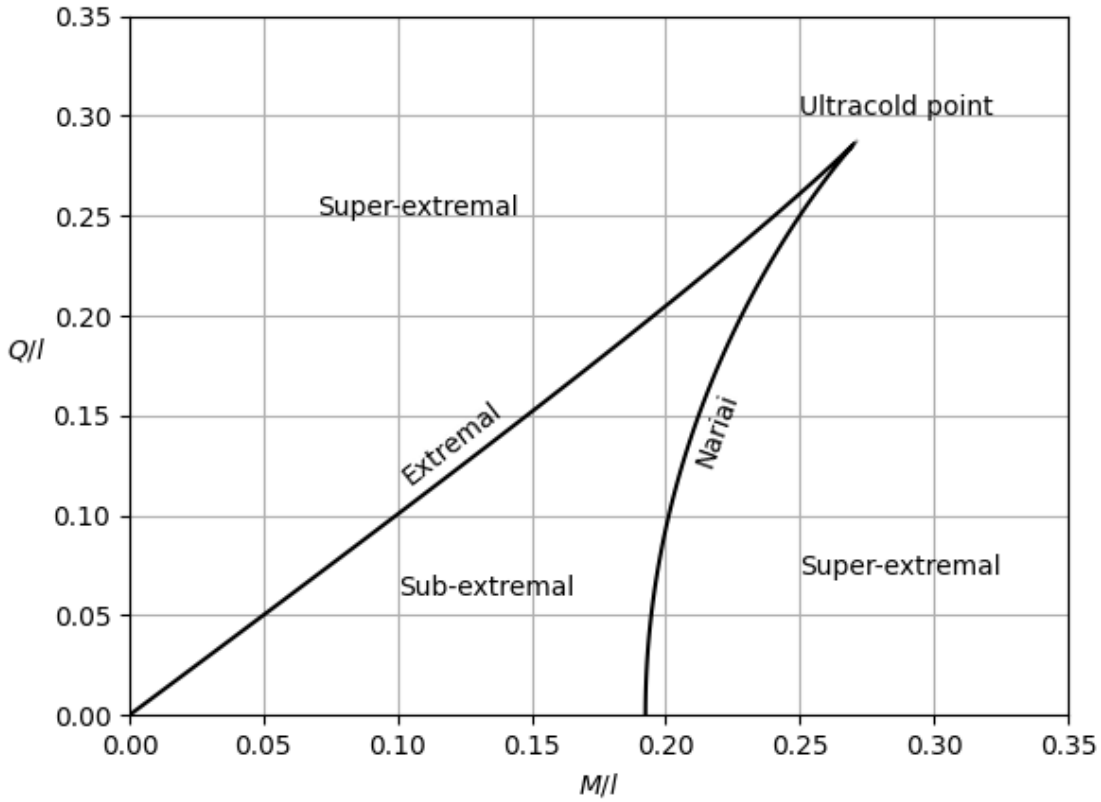

Figure 3.1: Phase diagram of RNdS. The upper branch is the extremal RNdS spacetime, for which $r_- = r_+ < r_c$. The lower branch is the Nariai branch, for which $r_< = r_+ = r_c$. The point where both branches meet is the ultra-cold black hole, for which $r_- = r_+ = r_c$.

The Einstein field equations then become

$$\tilde{R}_{ab} - \frac{1}{2}\tilde{R}\tilde{g}_{ab} + \Lambda\tilde{g}_{ab} = 8\pi\left(\epsilon\delta T^{\mathrm{q}}_{ab} + \tilde{T}^{\mathrm{cl}}_{ab}\right), \tag{3.19}$$

where $\delta T^{\mathrm{q}} = \langle\delta T\rangle$ signifies the matter content of the spacetime due to the presence of quantum fields in the curved spacetime and $\tilde{T}^{\mathrm{cl}}$ signifies the classical energy-momentum tensor, which is now varying due to the presence of the quantum perturbations. From this equation, it should be clear that we are doing semi-classical physics: we consider how quantum effects in the matter (the right-hand side of the Einstein field equations) backreact on the geometry (the left-hand side), but we do not include possible quantum properties of the geometry itself.

Expanding up to first order in the small quantity ϵ, we then get

$$\delta G_{ab} + \Lambda\delta g_{ab} = 8\pi\left(\delta T^{\mathrm{q}}_{ab} + \delta T^{\mathrm{cl}}_{ab}\right), \tag{3.20}$$

where in general (cf. [52])

$$\begin{aligned}\delta G_{ab} = -\frac{1}{2}\big[&\Box\delta g_{ab} + \nabla_b\nabla_a\delta g - \nabla^\mu\nabla_a\delta g_{b\mu} - \nabla^\mu\nabla_b\delta g_{a\mu} \\ &+ g_{ab}\left(\nabla^\mu\nabla^\nu\delta g_{\mu\nu} - \Box\delta g - R_{\mu\nu}\delta g^{\mu\nu}\right) + R\delta g_{ab}\big]\end{aligned} \tag{3.21}$$

and (cf. [69])

$$\begin{aligned}\delta T^{\mathrm{cl}}_{ab} = &\left(F_{\mu a}F_{\nu b} - \frac{1}{2}g_{ab}F_{\mu\rho}F_{\nu}{}^{\rho}\right)\delta g^{\mu\nu} - \frac{1}{4}F_{\mu\nu}F^{\mu\nu}\delta g_{ab} \\ &+ F^{\rho}{}_{b}\,\delta F_{\rho a} + F^{\rho}{}_{a}\,\delta F_{\rho b} - \frac{1}{2}g_{ab}F^{\mu\nu}\delta F_{\mu\nu}.\end{aligned} \tag{3.22}$$

We consider the spherically symmetric perturbation

$$\delta\,\mathrm{d}s^2 = \delta A(r,t_1)\,\mathrm{d}r^2 + \delta B(r,t_1)\,\mathrm{d}t^2\,. \tag{3.23}$$

Here, δA and δB depend on the 'slow' time scale

$$t_1 = \epsilon t. \tag{3.24}$$

We also consider the RNdS black hole charge and mass (and consequently also the blackening factor) to evolve on this slow time scale: $M = M(t_1)$, $Q = Q(t_1)$, and $f = f(r,t_1)$. Solving certain classes of differential equations through a naive perturbative approximation can lead to solutions that exhibit secular, unbounded growth where none is expected. The introduction of a slow time scale is a nice way of preventing such secular behaviour (cf. [36]). However, there may still be secular behaviour even at first order in ϵ, and so this analysis is expected to be good for $\epsilon t_1 \ll 1$ but not necessarily for t greater than that. If greater precision is required, it is possible to introduce a time scale $t_2 = \epsilon^2 t$, and so on.

In the case of spherically symmetric perturbations superimposed on the spherically symmetric RNdS spacetime, Eq. 3.21 simplifies considerably. Performing the calculations, it turns out that only the (t,r) component of the Einstein tensor contains time derivatives [38, 40], and thus is of greatest interest for our purposes. Explicitly [14],

$$\delta G_{tr} = \tilde{G}_{tr} = \tilde{R}_{tr} = \frac{2}{r}\partial_t\beta, \tag{3.25}$$

where

$$\beta = \frac{1}{2}\ln\left(\frac{1}{f(r,t_1)} + \epsilon\delta A\right). \tag{3.26}$$

Consequently,

$$\begin{aligned}\partial_t\beta &= \frac{1}{2\left(1+\epsilon f\delta A\right)}\left(-\frac{\dot{f}}{f} + \epsilon f\delta\dot{A}\right) \\ &= -\frac{1}{2}\frac{\dot{f}}{f} + \mathcal{O}\left(\epsilon^2\right),\end{aligned} \tag{3.27}$$

and thus

$$\delta G_{tr} = \frac{2\left(r\dot{M} - Q\dot{Q}\right)}{r\left(r^2 - 2Mr + Q^2 - r^4\right)} = -8\pi r^2\mathcal{T}, \tag{3.28}$$

where

$$\dot{M} = \frac{\mathrm{d}M}{\mathrm{d}t_1}(t_1)\bigg|_{t=0}, \quad \dot{Q} = \frac{\mathrm{d}Q}{\mathrm{d}t_1}(t_1)\bigg|_{t=0}, \tag{3.29}$$

and where we defined the mass-energy flux $\mathcal{T} = -\delta T^{\mathrm{q}}_{tr}/r^2$.

Similarly, perturbing the field strength tensor yields

$$\mathrm{d} \star \tilde{F} = \star \tilde{j}. \tag{3.30}$$

Since there is no classical current in the RNdS spacetime, this equation is equivalent to

$$\mathrm{d} \star \delta F = \star \delta j^{\mathrm{q}}. \tag{3.31}$$

The current density can be determined to be given by

$$\tilde{j} = \left(\rho(r), \frac{\mathcal{J}}{r^2}, 0, 0 \right), \tag{3.32}$$

where $\rho(r)$ is the charge density and $\mathcal{J}$ is a radially constant current. This was found using spherical symmetry and current conservation, $\nabla_\mu \tilde{j}^\mu = 0$, which is equivalent to $\partial_\mu \left(\sqrt{-g} \tilde{j}^\mu \right) = 0$ with $\sqrt{-g} = r^2 \sin\theta$. The charge Q of the RNdS black hole will change over time as

$$\dot{Q} = -\int_{S^2} \tilde{j}^r \sqrt{-g}\, \mathrm{d}\Omega = -4\pi \mathcal{J}. \tag{3.33}$$

Combining Eqs. 3.28 and 3.33, we find the following system of first-order ODEs:

$$\dot{Q} = -4\pi \mathcal{J}, \quad \dot{M} = -4\pi \left(r^4 f(r) \mathcal{T} + \frac{\mathcal{J} Q}{r} \right). \tag{3.34}$$

The quantity of interest in describing the path traced by the RNdS black hole through phase space is

$$\frac{\mathrm{d}M}{\mathrm{d}Q} = \frac{\dot{M}}{\dot{Q}} = r^4 f(r) \frac{\mathcal{T}}{\mathcal{J}} + \frac{Q}{r} \tag{3.35}$$

The task then remains to specify the mass-energy flux $\mathcal{T}$ and the electric current $\mathcal{J}$. For detailed expressions of these quantities, cf. [38, 40]; here, we only discuss the main ideas. First, the electric current is sourced by Schwinger pair production between the two horizons and is related to it by

$$\mathcal{J} \propto 2 \int_{r_+}^{r_c} \mathrm{d}r'\, r'^2 \Gamma(r'), \tag{3.36}$$

where the factor of 2 is due to the fact that particles are produced in pairs, one being attracted to and the other being repulsed by the charged black hole. The fact that the two produced particles move in opposite directions also means that the Schwinger current will not contribute to $\mathcal{T}$; this quantity is entirely due to Hawking radiation. The outer black hole horizon contributes an outgoing thermal flux of particles, and the cosmological horizon an incoming flux. Thus, up to an extra factor to account for the gravitational redshift, the mass-energy flux is given by the Stefan-Boltzmann law:

$$\mathcal{T} \propto \sigma \left(A_c T_c^4 - A_+ T_+^4 \right) \propto \frac{\sigma}{(4\pi)^3} \left(r_c^2 \left| f'(r_c) \right|^4 - r_+^2 \left| f'(r_+) \right|^4 \right), \tag{3.37}$$

where σ is the Stefan-Boltzmann constant and A_c and T_c are, respectively, the area and temperature of the cosmological horizon and analogously for the outer black hole horizon. We also used that $T_h = \kappa_h / 2\pi = f'(r_h)/4\pi$, where κ is the surface gravity [33, 57].

Combining the expressions for $\mathcal{T}$ and $\mathcal{J}$ with Eq. 3.35 leads to paths through phase space as illustrated in Fig. 3.2. From the plot, it is clear that these paths do not enter into forbidden super-extremal territory, as can also be shown more rigorously [40]. Moderately charged black holes first evolve toward thermal equilibrium ($Q = M$) before continuing to evaporate back to pure dS. The plot also shows the interesting phenomenon of anti-evaporation in the upper half of the diagram [11]. As expected, charged black hole evaporation in dS is well-behaved if the Schwinger rate is exponentially suppressed.

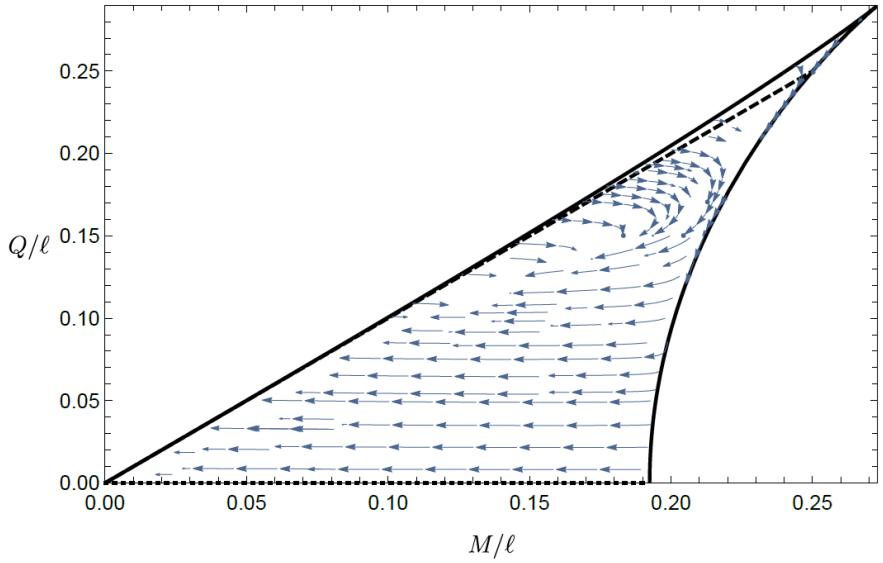

Figure 3.2: Paths traced through phase space by RNdS black holes under the combined influence of the Schwinger and Hawking effects. Note the anti-evaporation in the upper region of the phase diagram. Illustration adapted from [38].

Adiabatic regime ($m^2 \ll qE$)

In the adiabatic regime, we must take special care in invoking the Schwinger rate: the imaginary part of the effective action is no longer small, violating a key assumption in the derivation of the Schwinger rate (cf. Section 2.2). However, we will not need to work with the Schwinger rate directly. In this case, the electric field is so strong that the vacuum decay probability is close to 1, which means that this situation can be modelled as though the discharge happens instantaneously. The black hole sheds its charge immediately and is surrounded by charged particle-antiparticle pairs which annihilate and form a cloud of radiation.

In the adiabatic regime, the authors of [40] are primarily interested in what happens on the charged Nariai branch, since it is the evolution of these configurations that allows for the formulation of the Festina Lente bound. In the static patch coordinates of Section 3.2, the black hole horizon and cosmological horizon coincide on the Nariai branch of the black hole phase space. However, for an observer between these two horizons, the transition from a sub-extremal black hole to a charged Nariai black hole is perfectly regular: although the separation between the two horizons indeed decreases, they never cross. It is therefore assumed that the geometry of interest is $\mathrm{dS}_2 \times \mathrm{S}^2$, which is the near-horizon geometry of a Nariai-de Sitter black hole.

To allow for different species of energy in the universe, we will work with a generalised form of the Einstein-Maxwell theory given in Eq. 3.8:

$$S = \int \mathrm{d}^4x \sqrt{-g} \left[\frac{1}{16\pi} (R - 2\Lambda) - \mathcal{L} \right]. \tag{3.38}$$

For the same reason, we will not work directly with a dS metric: in dS, the only energy contribution comes from the cosmological constant. To capture the fact that in RNdS there will be an additional contribution in the form of radiation due to the rapid discharge of the black hole, we will work with an FLRW metric describing a homogeneous, isotropic, expanding universe:

$$\mathrm{d}s^2 = e^{-\phi(\tau)} \left(-\mathrm{d}\tau^2 + a^2(\tau)\, \mathrm{d}x^2 \right) + e^{2\phi(\tau)}\, \mathrm{d}\Omega_2^2 . \tag{3.39}$$

Inserting this metric into the action and using that $\sqrt{-g} = a e^{\phi} \sin\theta$, we find that

$$8\pi S = \int \mathrm{d}\Omega_2\, \mathrm{d}\tau\, \mathrm{d}x \left(-(e^{\dot{2}\phi})\dot{a} + e^{-\phi} a - 3 e^{\phi} a \right) - 8\pi \int \mathrm{d}\Omega_2\, \mathrm{d}\tau\, \mathrm{d}x\, a e^{\phi} \mathcal{L}, \tag{3.40}$$

where $\mathrm{d}\Omega_2 = \sin\theta\, \mathrm{d}\theta \wedge \mathrm{d}\phi$ (cf. [40] for details). The stress-energy tensor is defined as

$$T_{ab} = \frac{-2}{\sqrt{-g}} \frac{\delta S_M}{\delta g_{ab}}, \tag{3.41}$$

where $S_M = -\int \mathrm{d}\Omega_2\, \mathrm{d}V_2\, e^{\phi} \mathcal{L}$ refers to the matter component of the action. Consequently,

$$\begin{aligned} 8\pi \delta S_M &= 8\pi \int \mathrm{d}x^4\, \frac{\delta S_M}{\delta g^{\mu\nu}} \delta g^{\mu\nu} \\ &= -4\pi \int \mathrm{d}x^4\, \sqrt{-g} T_{\mu\nu} \delta g^{\mu\nu} \\ &= -4\pi \int \mathrm{d}\Omega_2\, \mathrm{d}\tau\, \mathrm{d}x\, a e^{\phi} T_{\mu\nu} \delta g^{\mu\nu}. \end{aligned} \tag{3.42}$$

Moreover,

$$\delta g^{ab} = \frac{\delta g^{ab}}{\delta a} \delta a + \frac{\delta g^{ab}}{\delta \phi} \delta\phi = -2 \frac{e^{\phi}}{a^3} \delta^{a,x} \delta^{b,x} \delta a + \left(3 e^{\phi} g_2^{ab} - 2 g^{ab} \right) \delta\phi, \tag{3.43}$$

where g_2 represents the two-dimensional metric $\mathrm{d}s_2^2 = -\mathrm{d}\tau^2 + a^2\, \mathrm{d}x^2$. Varying the action with respect to a and to ϕ, we find the following equations of motion:

$$\begin{cases} \ddot{(r^2)} = 3r - \frac{1}{r} - 8\pi \frac{r^2}{a^2} T_{xx} \\ 2r^2 \frac{\ddot{a}}{a} = \frac{1}{r} + 3r + 4\pi r \left(3T_2 - 2T \right) \end{cases}, \tag{3.44}$$

where we introduced $r = e^{\phi}$ and $T_2 = T_{\mu\nu} e^{\phi} g_2^{\mu\nu}$. In the context of a rapidly discharging RNdS black hole, all energy is of electromagnetic origin, so the stress-energy tensor is traceless ($T = 0$). Due to the spherical symmetry of the system, the stress-energy tensor can be decomposed as follows:

$$T_{ab} = \rho u_a u_b + p_1 \gamma_a \gamma_b + p_2 g_{ab}^{\Omega}, \tag{3.45}$$

where u^μ is a unit vector in the τ-direction, γ^μ is a unit vector in the x-direction, and $g^\Omega_{\mu\nu}$ is the metric on the two-sphere. The tracelessness of the stress-energy tensor implies $\rho = p_1 + 2p_2$. Using these relations, the equations of motion can be rewritten as

$$\begin{cases} \ddot{(r^2)} = 3r - \frac{1}{r} - 8\pi r p_1 \\ 2r^2 \frac{\ddot{a}}{a} = \frac{1}{r} + 3r + 12\pi r \left(p_1 - \rho\right) \end{cases}. \tag{3.46}$$

As before, once the equations of motion are derived, it is time to specify the spacetime's energy content. The adiabatic regime is modelled by assuming that at $t = 0$, the electric field and charge are instantly transformed into pure radiation, without any loss of energy. Using Gauss's law for the electric field $E(r)$ sustained by a point charge Q, the energy density ρ is found to satisfy

$$8\pi\rho = E^2(r) = \frac{Q^2}{r^4}. \tag{3.47}$$

Moreover,

$$p_1 = \alpha\rho, \quad p_2 = \beta\rho, \quad \alpha + 2\beta = 1 \tag{3.48}$$

where, because we are now working with radiation, α and β are positive parameters whose precise values are dictated by the interactions between the charged particles emitted. If we assume that these interactions are very efficient and that the system quickly thermalises locally, it makes sense to assume isotropy and fix $\alpha = \beta = 1/3$. The conservation of stress-energy ($\nabla_\nu T^{\mu\nu} = 0$) then implies that

$$\dot{\rho} + \rho\left(2\dot{\phi} + \frac{4}{3}\frac{\dot{a}}{a}\right) = 0, \tag{3.49}$$

and after integrating, we find that

$$\rho = \rho_0 e^{-2\phi} a^{-4/3}, \quad 8\pi\rho_0 = \frac{Q_0^2}{r_0^2}, \tag{3.50}$$

where Q_0 and r_0 are the initial charge and black hole radius and $a_0 = 1$. Finally, introducing $s = r^2$ and using Eq. 3.50, we find the following equations of motion in the adiabatic regime:

$$\begin{cases} \ddot{s} = 3\sqrt{s} - \frac{1}{\sqrt{s}}\left(1 + \frac{8\pi}{3}\frac{\rho_0}{a^{4/3}}\right) \\ \frac{\ddot{a}}{a} = \frac{1}{2s^{3/2}}\left(1 + 3s - 8\pi\frac{\rho_0}{a^{4/3}}\right) \end{cases}. \tag{3.51}$$

For Nariai black holes, the following condition always holds (cf. Section 4.2.2):

$$8\pi\rho_0 = \frac{Q_0^2}{r_0^2} < 1. \tag{3.52}$$

Consequently, the equation of motion for a implies that the expansion is always accelerating. Similarly, since Nariai black holes always satisfy $s \leq 1/3$ (where the upper bound corresponds to the chargeless limit, again cf. Section 4.2.2), $\ddot{s} < 0$ at all times. Moreover, since $\dot{s}(0) = 0$, $\dot{s} < 0$ at all subsequent times. Thus, the two-sphere is always shrinking. As time progresses, $\rho_0/a^{4/3} \to 0$. Physically, the radiation is diluted away by the redshift caused by the expansion of the universe. Consequently, the equation of motion for s can be integrated to yield a first integral K:

$$\frac{1}{2}\dot{s}^2 + V(s) = K, \tag{3.53}$$

where we defined the effective potential $V(s)$ as

$$V(s) = 2\sqrt{s}(1-s). \tag{3.54}$$

A plot of $V(s)$ can be found in Fig. 3.3. The effective potential reaches a maximum at $s = 1/3$, but the initial configuration is always to the left of this point and subsequently moves to the left; that is, toward $s = 0$.

Thus, putting all pieces together, the two-sphere collapses (meaning that the black hole curvature becomes enormous), while the cosmic scale factor a blows up. This scenario corresponds to a Big Crunch: due to the near-instantaneous evaporation of the black hole's charge, the black hole enters the forbidden region of phase space, becoming super-extremal with a mass higher than that of a neutral Nariai black hole (cf. Fig. 3.1). In a sense, the black hole quickly annexes the entire static patch into its interior. Observers previously between the black hole horizon and the cosmological horizon now look forward to a crunch singularity. It can be shown more rigorously that this Big Crunch is guaranteed by a singularity theorem and is therefore truly unavoidable [40].

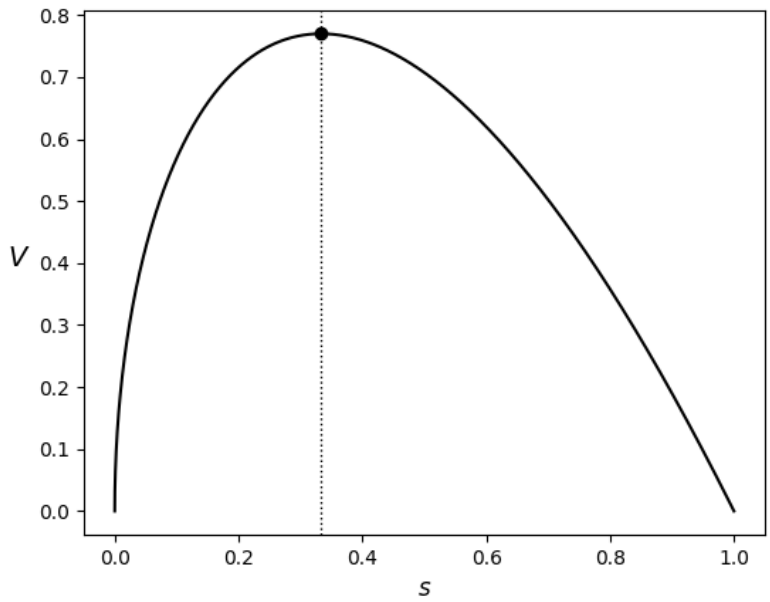

Figure 3.3: The effective potential $V(s)$. Since the starting configuration lies to the left of the maximum at $s = 1/3$ and $\dot{s} < 0$ for all subsequent times, the geometry is driven to $s = 0$. Figure reconstructed from [40].

3.3 Festina Lente and the swampland

We are now finally in a position to formulate the Festina Lente (FL) conjecture. The evaporation of charged black holes in the adiabatic regime evidently leads to pathological spacetimes sporting naked singularities and exhibiting crunching behaviour. There are many sensible reasons to want to avoid such pathologies (cf. [40] for details). Logically, there is only a limited set of ways to do so. First, the Big Crunch might be circumvented by

an as yet unknown quantum gravitational process which transforms the RNdS spacetime into an empty dS spacetime. This solution shows some similarities to arguments against the WCCC; perhaps there is no fundamental rule against naked singularities, as they might be protected by physics at the level of quantum gravity. Although some such mechanisms have been found in string theory (cf. [31] for some references), this first possibility remains quite speculative. Secondly, perhaps charged black holes cannot exist if particles exist within the adiabatic regime. However, semi-classically, there does not seem to be any reason why we should not be able to smoothly deform any configuration within the shark fin (including empty dS, cf. Fig. 3.1) into a charged Nariai configuration.

Consequently, we are left only with the third option: to bar the possibility of a Big Crunch, we have to prohibit the existence of particles in the adiabatic regime. In other words, the evolution of RNdS black holes has phenomenological consequences for particle physics and gives us a good argument to limit its parameter space. Concretely, to avoid the adiabatic regime, we should impose the following constraint on all particle species[1]:

$$m^2 \gtrsim qH. \tag{3.55}$$

This result was found using the fact that the electric field is largest for the ultra-cold configuration and several other facts (cf. Section 4.2), such as that in this configuration $r_u^2 = l^2/6$, that $H = l^{-1}$ and that

$$E_u^2 = \frac{Q_u^2}{r_u^4} = \frac{1}{r_u^2} - \frac{3}{l^2} = 3H^2. \tag{3.56}$$

Since the inequality Eq. 3.55 avoids the ultra-fast discharge of charged black holes and consequently also the occurrence of a Big Crunch in RNdS spacetime, it is called the Festina Lente bound: charged black holes should be able to evaporate back to empty dS space, but should not be rushed to do so.

The FL proposal is part of a wider collection of claims collectively called the *swampland conjectures*. The idea behind the swampland programme goes as follows (cf. [39] for a nice review). Physicists expect there to be a physical theory that correctly describes our universe, that is valid at both high and low energies, and in which gravity is treated on the same footing as the other forces of nature. In short, a theory of quantum gravity. String theory is the main candidate for a theory of quantum gravity today. However, string theory has an extremely large number of solutions, and it is near impossible to find the one that corresponds to our universe through a direct search. Yet, it also seems to be the case that not just any low-energy effective field theory (EFT) can be incorporated into a theory of quantum gravity. In other words, the existence of a theory of quantum gravity constrains the form that theories at low energy can take. Discovering these constraints would provide us with a lot of physical information and would allow us to separate the string *landscape* of allowed solutions from the *swampland* of EFTs that cannot be coupled to a theory of quantum gravity. Often, swampland conjectures find their origin in thought experiments featuring black holes. Both the WCCC and the FL conjecture are examples of conjectures inspired by black hole physics.

However, some authors have raised questions about the conclusions of [40]. The calculations of [40] in the adiabatic regime assumed that a two-dimensional near-horizon

[1] In more dimensionful units, this constraint can be written as $m^2 \gtrsim qgM_PH$, where g is the gauge coupling constant and $M_P = (8\pi G)^{-1/2}$ is the Planck mass.

approximation to the Nariai geometry is sufficient to capture the essential physics of black hole decay. In [1], the question is raised if this assumption is justified; a quantum tunnelling perspective is used to calculate the black hole decay directly from the four-dimensional theory, and it is found that including higher-order backreactions might avoid the Big Crunch.

In a similar vein, the authors of [37] argue that it is important to take into account the spatial profile of the Schwinger effect. If the Compton wavelength λ of the produced particles is small compared to the horizon separation ($\lambda = m^{-1} < r_c - r_+$), the particles are produced close to the black hole horizon, the Schwinger effect is suppressed, and no Big Crunch occurs, consistent with the results of [40] in the quasi-static regime. However, if λ is large compared to the horizon separation ($\lambda > r_c - r_+$, i.e. in the adiabatic regime), particles can be produced in appreciable numbers outside of the cosmological horizon, meaning that the black hole mass and charge should receive significant corrections due to the discharge, which might offer a way out of the Big Crunch in the adiabatic regime.

Although these remarks by [37] do not seem unreasonable, they are not supported by any evidence in asymptotically dS RN spacetime, but are based solely on the calculations in asymptotically flat RN spacetime we exhibited in Chapter 2. Thus, it remains an open task to calculate the spatial profile of the Schwinger effect in RNdS spacetime, a task that we will tackle in Chapter 4.

Conclusion

This chapter was entirely devoted to the analysis of the RNdS spacetime, with special attention to its semi-classical evolution under the influence of the Schwinger effect. Surprisingly, it was found that, in a sense, charged Nariai black holes shed their charge too quickly if our theory contains charged particles whose mass is too small; almost immediately, their mass becomes too great for the dS background to contain it, leading to a pathological spacetime exhibiting a Big Crunch. Given the assumptions made in this regime, this crunching behaviour is a robust prediction, which led the authors of [40] to postulate the FL bound. Some authors have raised doubts concerning some of the assumptions made in the derivation of the FL bound, which calls for a more careful do-over of the derivation that led to this proposal, ideally using different methods. Therefore, in Chapter 4, we will make an attempt at applying the machinery of Chapter 2 to the context of extremal and Nariai RNdS black holes.

Chapter 4

Schwinger effect in Reissner-Nordström-de Sitter spacetime

Introduction

In the earlier chapters of this dissertation, we studied QFTCS in general, next described a clever way of calculating the Schwinger rate in RN spacetime, and finally saw how an explosive Schwinger effect in a Nariai RNdS spacetime could have catastrophic consequences for the spacetime as a whole. These discussions find their culmination in this fourth, and final, chapter, in which we apply the formalism of Chapter 2 to the case of extremal and Nariai RNdS spacetimes, in hopes of gaining a better understanding of the Schwinger effect and FL bound in these spacetimes.

The chapter is organized as follows. In Section 4.1, we extend the treatment of Section 2.4.1 to spacetimes that are not Ricci-flat ($R \neq 0$). Then, in Section 4.2, we apply the formalism first to extremal RNdS black holes, and secondly to Nariai RNdS black holes. As we will see, our results in this chapter are in agreement with the results of Chapter 2 for small extremal black holes, but are rather harder to interpret for larger extremal black holes and charged Nariai black holes.

4.1 Worldlines for non-zero Ricci scalar

To calculate the Euclidean effective action in RNdS spacetime, we go through the same steps as in Chapter 2. We again study scalar QED, but now, since the spacetime is asymptotically dS, we must account for the fact that the Ricci scalar does not vanish. To do so, we add an explicit coupling to the gravitational field in the action:

$$S[\phi, \phi^*] = \int \mathrm{d}^4x \, \sqrt{-g} \frac{1}{2} \phi^* H_{A,R} \phi, \tag{4.1}$$

where $H_{A,R} = D_\mu D^\mu - m^2 - \xi R$ and $D_\mu = \nabla_\mu + ieA_\mu$. As before, we take the gauge field and the spacetime to be fixed. This also means that we will set any derivative of R to zero. Moreover, we assume that $R(x)$ is a constant throughout the spacetime, since our

focus is on de Sitter spacetime. We find that

$$S^E_{\text{eff}} = -\frac{1}{2}\int_0^\infty \frac{\mathrm{d}s}{s}\int \mathrm{d}^4x_0\,\sqrt{-g}\langle x_0|e^{-sH_{A,R}}|x_0\rangle \tag{4.2}$$

and

$$\langle x_0|e^{-sH_{A,R}}|x_0\rangle = \int_{x(T=0)=x_0}^{x(T=s)=x_0}\mathcal{D}x e^{-\int_0^s \mathrm{d}T\left[\frac{1}{4}\dot{x}_\mu\dot{x}^\mu + eA_\mu\dot{x}^\mu + m^2 + \xi R\right]}. \tag{4.3}$$

Define $\tilde{m} = \sqrt{m^2+\xi R}$. By rescaling $s = \frac{s'}{\tilde{m}^2}$ and $T = \frac{s'}{\tilde{m}^2}T'$, the worldline action can be rewritten as

$$S_{\text{wl}}[s,x] = \int_0^1 \mathrm{d}T\left(\frac{\tilde{m}^2}{4s}\dot{x}_\mu\dot{x}^\mu + eA_\mu\dot{x}^\mu + s\right), \tag{4.4}$$

and the Euclidean effective action as

$$S^E_{\text{eff}} = -\frac{1}{2}\int_0^\infty \frac{\mathrm{d}s}{s}\int \mathrm{d}^4x_0\,\sqrt{-g}\int_{x(0)=x_0}^{x(1)=x_0}\mathcal{D}x e^{-\int_0^1 \mathrm{d}T\left(\frac{\tilde{m}^2}{4s}\dot{x}_\mu\dot{x}^\mu + eA_\mu\dot{x}^\mu + s\right)}. \tag{4.5}$$

The analysis now proceeds exactly the same as in Sections 2.4.1 and 2.4.2, and the results are the same as well, except that the particle mass is now corrected with a term dependent on the cosmological constant. This makes sense intuitively: in an expanding universe, mass seems to gain extra inertia. The expansion of the worldline action up to second order can be found in Appendix A. For convenience, we list the most important equations:

$$\begin{cases} g_{\mu\nu}\dot{\bar{x}}^\mu\dot{\bar{x}}^\nu = a^2 \\ \bar{s} = \frac{\tilde{m}a}{2} \\ \omega = \frac{\tilde{m}}{a}g_{00}\dot{x}^0 + ex^1\partial_{x^1}A_0 \\ \dot{x}^1 = \pm a\sqrt{g_{11}^{-1}\left[1 - \frac{(ex^1\partial_{x^1}A_0-\omega)^2}{\tilde{m}^2 g_{00}}\right]} \\ S_{\text{wl}}[\bar{s},\bar{x}] = \int_0^1 \mathrm{d}T\left(\frac{\tilde{m}^2}{4\bar{s}}\dot{\bar{x}}_\mu\dot{\bar{x}}^\mu + eA_\mu\dot{\bar{x}}^\mu + \bar{s}\right) \end{cases}. \tag{4.6}$$

Note that we have slightly generalised the expressions for ω and the radial equation to allow for more general expressions of the four-potential A, which we will need in our discussion of charged Nariai black holes in Section 4.2.2.

4.2 Instantons in Reissner-Nordström-de Sitter

Now, let us see if we can derive anything about the Schwinger rate in RNdS spacetime, which we analysed in Section 3.2. We are specifically interested in the limits where two of the three horizons coincide, since these spacetimes are structurally simpler than a generic RNdS spacetime and are of interest in the context of the FL bound (cf. Section 3.3). More precisely, we want to calculate S_{wl} using an algorithm similar to the one we used in Section 2.4.2. However, the specifics depend on which degenerate limit (extremal or Nariai) is taken, so we will consider both cases separately.

4.2.1 Extremal Reissner-Nordström-de Sitter

For an extremal RNdS black hole (and, as it turns out, for a charged Nariai black hole), the blackening factor (cf. Eq. 3.13) reduces to [57]

$$f(r) = \left(1 - \frac{r_E}{r}\right)^2 \left(1 - \frac{r^2}{l^2} - 2\frac{r_E r}{l^2} - 3\frac{r_E^2}{l^2}\right), \tag{4.7}$$

where $r_E = r_+ = r_-$ denotes the radius of the degenerate horizon. The mass M_E, charge Q_E and cosmological constant l of the spacetime are related by [10]

$$Q_E^2 = r_E^2 \left(1 - 3\frac{r_E^2}{l^2}\right), \quad M_E = r_E \left(1 - 2\frac{r_E^2}{l^2}\right). \tag{4.8}$$

The degenerate horizon radius r_E is bounded from below by the black hole singularity and bounded from above by the cosmological horizon r_c, which can be calculated as the positive root of

$$1 - \frac{r^2}{l^2} - 2\frac{r_E r}{l^2} - 3\frac{r_E^2}{l^2} = 0. \tag{4.9}$$

Explicitly:

$$r_c = -r_E + l\sqrt{-2\frac{r_E^2}{l^2} + 1}. \tag{4.10}$$

As r_E inflates, r_c is pulled in. Demanding $0 \leq r_E < r_c$, one finds that r_E satisfies $0 \leq r_E < l/\sqrt{6} \approx 0.41$. A plot of M_E, Q_E, and Q_E/M_E as a function of r_E can be found in Fig. 4.1. As expected, higher values of l (i.e. lower values of the cosmological constant) allow for larger black hole radii, masses, and charges. Moreover, for black hole radii that are small compared to the cosmological horizon ($r_E \ll l/\sqrt{6}$), the charge-to-mass ratio stays close to the asymptotically flat RN value of 1; small black holes do not feel much difference between asymptotically flat and asymptotically de Sitter spacetimes.

The radial instanton equation Eq. 2.36 for extremal RNdS is

$$\dot{r} = \pm a\sqrt{f(r) - \frac{e^2}{\tilde{m}^2}\left(\frac{Q_E}{r} - \frac{\omega}{e}\right)^2}. \tag{4.11}$$

To simplify, we define $z = e/\tilde{m}$ and $\rho_0 = \omega/e$. Note that, contrary to the case of asymptotically flat RN, z and ρ_0 in RNdS implicitly depend on l through their dependence on $\tilde{m}$. However, this should not worry us too much. We can still regard

$$z = \frac{e}{\sqrt{m^2 + \xi\frac{12}{l^2}}} \tag{4.12}$$

as an essentially free parameter. It is just that the particles involved in strongly cosmologically curved spacetimes will need small masses or large charges to counterbalance the effect of the l-dependent term. We also introduce a new radial coordinate $\rho = r_E/r$, which maps the region outside the degenerate horizon to $(0, 1)$. The cosmological horizon is located at $\rho_c = r_E/r_c$.

We then find that

$$\dot{\rho} = \mp\frac{a}{r_E}\rho\sqrt{h(\rho)}, \tag{4.13}$$

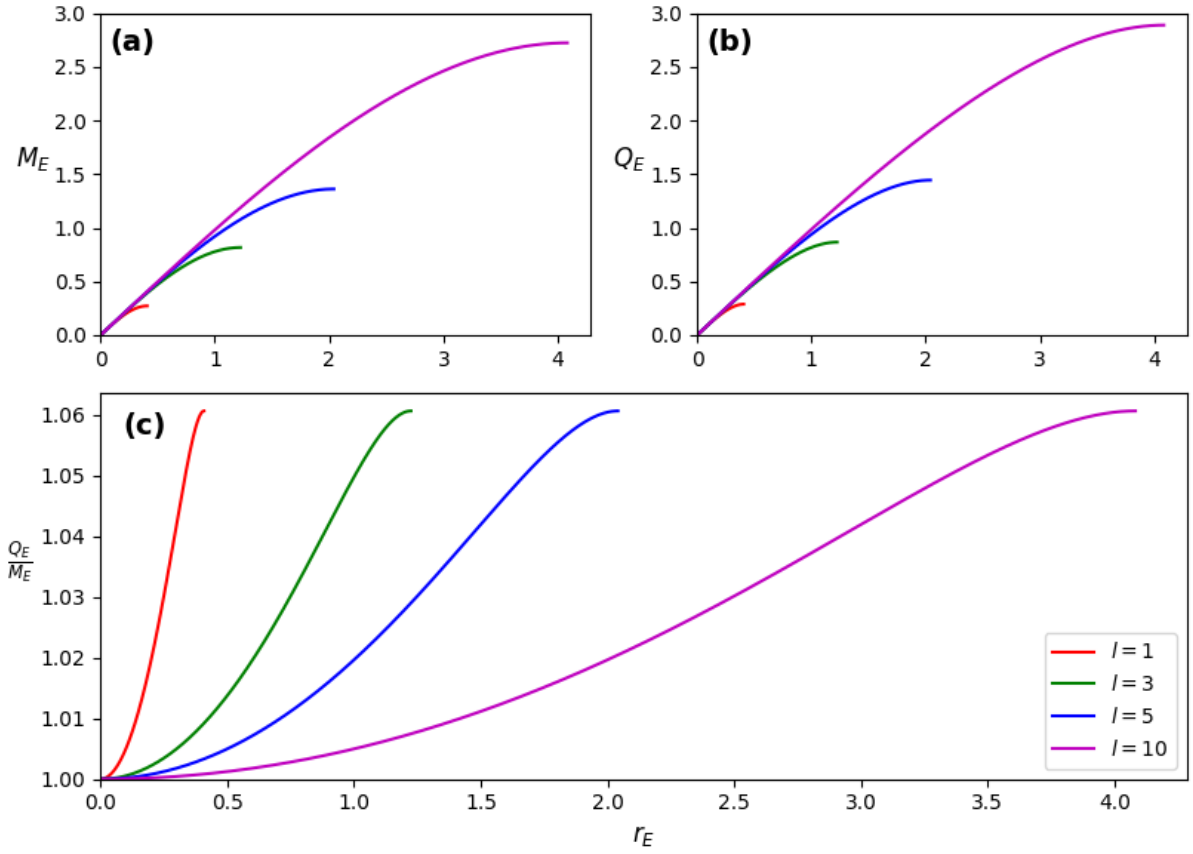

Figure 4.1: (a) Mass M_E, (b) charge Q_E, and (c) charge-to-mass ratio Q_E/M_E for an extremal RNdS black hole as a function of the degenerate horizon radius r_E for different values of the cosmological constant.

with an effective potential given by

$$h(\rho) = A\rho^4 + B\rho^3 + C\rho^2 + E, \tag{4.14}$$

where we defined

$$\begin{cases} A = 1 - \frac{Q_E^2}{r_E^2} z^2 - 3\frac{r_E^2}{l^2} \\ B = 2\left(\frac{Q_E}{r_E} z^2 \rho_0 - 1 + 2\frac{r_E^2}{l^2}\right) \\ C = 1 - z^2\rho_0^2 \\ E = -\frac{r_E^2}{l^2} \end{cases}. \tag{4.15}$$

This reduces neatly to Eq. 2.41 in the asymptotically flat limit ($r_E/l \to 0$). Solving the radial equation Eq. 4.13 analytically would result in an elliptic integral [13], but the analytic solution is not of real interest to us here. Similarly as in Section 2.4.2, we find that

$$\dot{\tau} = \frac{az}{f(\rho)}\left(\rho_0 - \frac{Q_E}{r_E}\rho\right) \tag{4.16}$$

and

$$\frac{\mathrm{d}\tau}{\mathrm{d}\rho} = \frac{z r_E \left(\rho_0 - \frac{Q_E}{r_E}\rho\right)}{\rho f(\rho)\sqrt{h(\rho)}}. \tag{4.17}$$

Again we impose the looping behaviour through the following conditions:

$$\begin{cases} \rho(T=0) = \rho(T=1) = \rho_\times \\ \rho(T=\frac{1}{2}) = \rho_2 \\ \tau(T=0) = \tau(T=\frac{1}{2}) = 0 \end{cases} . \tag{4.18}$$

The worldline instanton action is now given by

$$\begin{aligned} S_{\text{wl}}[\bar{s},\bar{x}] &= \tilde{m}a + e\int_0^1 \mathrm{d}T\, A_0\dot{\tau} \\ &= \tilde{m}\left[a + Q_E z^2 \times 2I\right], \end{aligned} \tag{4.19}$$

where

$$I = \int_{\rho_\times}^{\rho_2} \mathrm{d}\rho\, \frac{\rho_0 - \frac{Q_E}{r_E}\rho}{f(\rho)\sqrt{h(\rho)}}. \tag{4.20}$$

The algorithm of Section 2.4.3 is then adapted as follows. Without loss of generality, we fix $l = 1$, since the only quantity of interest is the ratio r_E/l. Fixing l allows us to constrain r_E. Choosing an allowed black hole size r_E subsequently allows us to calculate Q_E and M_E. Then we choose some z of interest. Finally, we select those ρ_0 that allow for two distinct real zeros of $h(\rho)$ in the interval $(0, 1)$. This requirement ensures the existence of instanton loops. For each such ρ_0, we determine $\rho_\times$ and a, and finally compute I and $S_{\text{wl}}[\bar{s},\bar{x}]$.

Applying this algorithm, we produced Figs. 4.2 and 4.3, which show an excellent agreement with the results of Section 2.4.3 in the small black hole limit. However, as we increase r_E, the $\mathrm{AdS}_2\times\mathrm{S}^2$ near-horizon approximation becomes increasingly worse. This is no surprise, since the near-horizon geometry close to the ultra-cold point is no longer $\mathrm{AdS}_2\times\mathrm{S}^2$ (cf. Section 3.2). Interestingly, from Fig. 4.4 we notice that for high z and large r_E, the worldline action becomes negative, indicating a strong Schwinger effect. This is in agreement with the results of Section 3.2.3 in the adiabatic regime. However, surprisingly, the action becomes even more negative near the cosmological horizon. This would mean that the Schwinger effect is actually most pronounced near r_c. Without other, more established results to compare to, it is hard to determine whether this result is reliable or suggests a breakdown of the numerical solver. For example, similar to the AdS_2 approximation near the black hole horizon, an approximation of the worldline instanton action near the cosmological horizon would constitute an independent test of our results. We are not aware of such results in the current literature. In the case where our results near the cosmological horizon turn out to be numerical artefacts (which seems quite possible given the other strange behaviour visible in Fig. 4.4), a more careful approach could be to consider the region near the cosmological horizon (where the geometry is approximately $\mathrm{Rind}_2\times\mathrm{S}^2$ [63]) independently from the rest of the static patch. Afterwards, the results from these calculations can be stitched together with the results from the rest of the spacetime, a task we leave for future work.

4.2.2 Nariai Reissner-Nordström-de Sitter

In the Nariai limit of the RNdS spacetime, the degenerate horizon radius r_N is bounded from below by the inner black hole horizon and bounded from above by the requirement

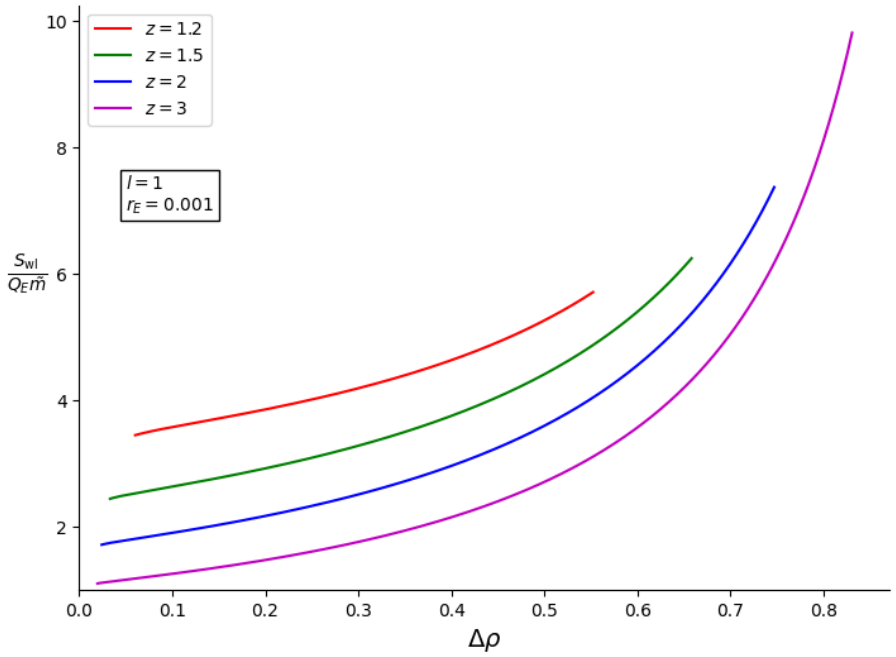

Figure 4.2: Radial profile of the worldline action between the outer black hole horizon r_E and the cosmological horizon r_c for small extremal RNdS black holes (i.e. $r_E/l \ll 1$). Excellent correspondence is found with extremal RN black holes in asymptotically flat spacetime.

that the solutions of the quadratic in the blackening factor not be complex. Physically, this is the requirement that there be a third horizon. The result is that r_N satisfies $\frac{l}{\sqrt{6}} < r_N \leq \frac{l}{\sqrt{3}}$. The lower bound corresponds to the ultra-cold point, and the upper bound corresponds to the uncharged Nariai configuration. A plot of M_N, Q_N, and Q_N/M_N as a function of r_N can be found in Fig. 4.5. Higher values of l again allow for larger black holes. As a charged Nariai black hole becomes large compared to the inner black hole horizon ($r_N \gg r_-$), its charge tends to zero ($Q_N \to 0$). Rather counterintuitively, M_N also decreases as r_N grows. However, this can be understood as follows: if the black hole mass decreases, spacetime as a whole is less deformed by its presence, meaning that the (degenerate) cosmological horizon can relax outward.

In our investigations so far, we have been interested in the Schwinger rate as measured by an observer between the outer black hole horizon and the cosmological horizon. In the coordinate system that we have been using until now, these two horizons seem to collide in the Nariai limit. However, using a suitable coordinate transformation, it can be shown that the two horizons do not coincide, even though their separation decreases [40]. Concretely, in the near-horizon limit, the Lorentzian metric and electric four-potential become

$$\mathrm{d}s^2 = l_{\mathrm{dS}}^2 \left(\rho^2 \, \mathrm{d}t^2 - \frac{\mathrm{d}\rho^2}{\rho^2} \right) + r_N^2 \, \mathrm{d}\Omega_2^2, \quad A = -Q_N \frac{l_{\mathrm{dS}}^2}{r_N^2} \rho \, \mathrm{d}t, \tag{4.21}$$

where

$$l_{\mathrm{dS}}^2 = \frac{r_N^2 l^2}{6r_N^2 - l^2}. \tag{4.22}$$

This corresponds to a $\mathrm{dS}_2 \times \mathrm{S}^2$ spacetime. Through a suitable coordinate transformation

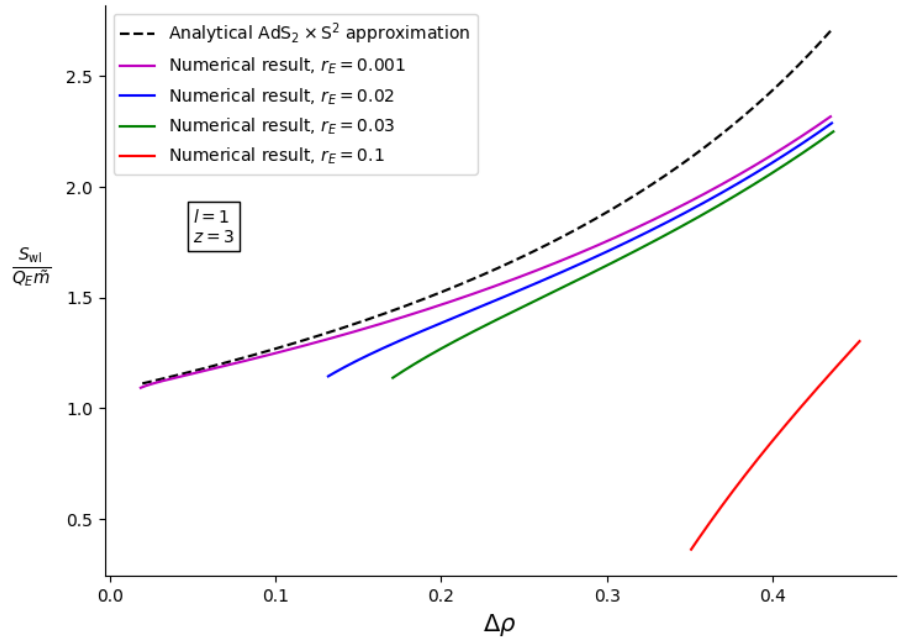

Figure 4.3: Radial profile of the worldline action close to the degenerate horizon r_E for increasingly large extremal RNdS black holes. As the black hole becomes larger, the near-horizon geometry is no longer well-approximated by $\mathrm{AdS}_2 \times \mathrm{S}^2$.

and Wick rotation [10], these can be turned into a Euclidean metric and four-potential:

$$\mathrm{d}s^2 = l_{\mathrm{dS}}^2 \left(\sin^2\chi\,\mathrm{d}\tau^2 + \mathrm{d}\chi^2\right) + r_N^2\,\mathrm{d}\Omega_2^2, \quad A = A_0(\chi)\,\mathrm{d}\tau = -Q_N \frac{l_{\mathrm{dS}}^2}{r_N^2}\cos\chi\,\mathrm{d}\tau, \tag{4.23}$$

which is an $\mathrm{S}^2 \times \mathrm{S}^2$ with respective radii l_{dS} and r_N. The black hole horizon lives at $\chi = 0$, and the cosmological horizon at $\chi = \pi$.

In these coordinates, the instanton paths are determined by

$$\begin{cases} \dot{\tau} = az\frac{\chi_0 - \chi\partial_\chi A_0}{g_{00}} = az\frac{\chi_0 - \chi\partial_\chi A_0}{l_{\mathrm{dS}}^2 \sin^2\chi} \\ \dot{\chi} = \pm a\sqrt{g_{11}^{-1}\left(1 - z^2\frac{(\chi\partial_\chi A_0 - \chi_0)^2}{g_{00}}\right)} = \pm\frac{a}{l_{\mathrm{dS}}^2\sin\chi}\sqrt{h(\chi)} \end{cases}, \tag{4.24}$$

where we defined $z = e/\tilde{m}$, $\chi_0 = \omega/e$, and

$$h(\chi) = l_{\mathrm{dS}}^2 \sin^2\chi - z^2\left(Q_N\frac{l_{\mathrm{dS}}^2}{r_N^2}\chi\sin\chi - \chi_0\right). \tag{4.25}$$

Moreover,

$$\frac{\mathrm{d}\tau}{\mathrm{d}\chi} = \pm z\frac{\chi_0 - \chi\partial_\chi A_0}{\sin\chi\sqrt{h(\chi)}}. \tag{4.26}$$

As before, the instanton paths are subject to the following conditions:

$$\begin{cases} \chi(T=0) = \chi(T=1) = \chi_\times \\ \chi(T=\frac{1}{2}) = \chi_2 \\ \tau(T=0) = \tau(T=\frac{1}{2}) = 0 \end{cases}. \tag{4.27}$$

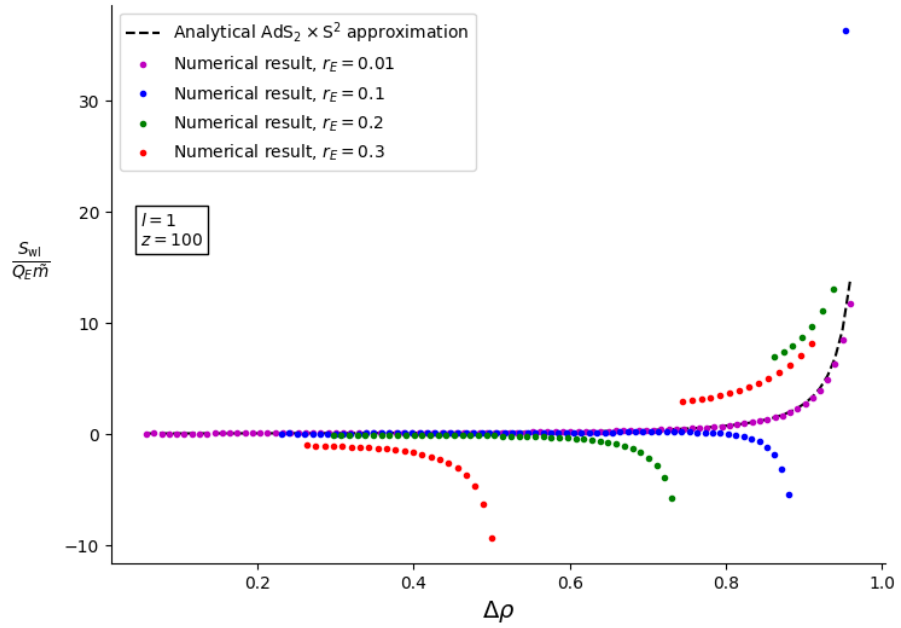

Figure 4.4: Radial profile of the worldline action between outside the outer black hole horizon r_E for $z = 100$ and for large extremal RNdS black holes. As r_E grows, r_c shrinks. The worldline action becomes negative, and increasingly so near the cosmological horizon. This implies an explosive Schwinger effect near r_c, a result to be taken with a grain of salt. The numerical solver only finds results outside of a certain interval around r_c. This erratic behaviour suggests the breakdown of our numerical solver.

The worldline instanton action is given by

$$\begin{aligned} S_{\mathrm{wl}}[\bar{s}, \bar{x}] &= \tilde{m} a + e \int_0^1 \mathrm{d}T \, A_0 \dot{\tau} \\ &= \tilde{m} \left[a - Q_N \frac{l_{\mathrm{dS}}^2}{r_N^2} z^2 \times 2I \right], \end{aligned} \tag{4.28}$$

where

$$I = \int_{\chi_\times}^{\chi_2} \mathrm{d}\chi \cot\chi \frac{\chi_0 - \chi \partial_\chi A_0}{\sqrt{h(\chi)}}. \tag{4.29}$$

However, the numerical solver was not able to compute the action on the basis of these equations. Quite possibly, our algorithm has at this point become too prone to numerical errors for it to be of use. Consequently, other methods have to be found to make progress in computing the radial profile of the Schwinger effect in the Nariai limit of RNdS black holes.

Conclusion

In this chapter, we attempted to apply the methods of Chapter 2 to RNdS spacetime. This attempt was successful in the case of small extremal RNdS black holes, but less so for larger extremal black holes and Nariai black holes. The reason for this is quite likely that the numerical solver that we have used is not sensitive enough to these more complex

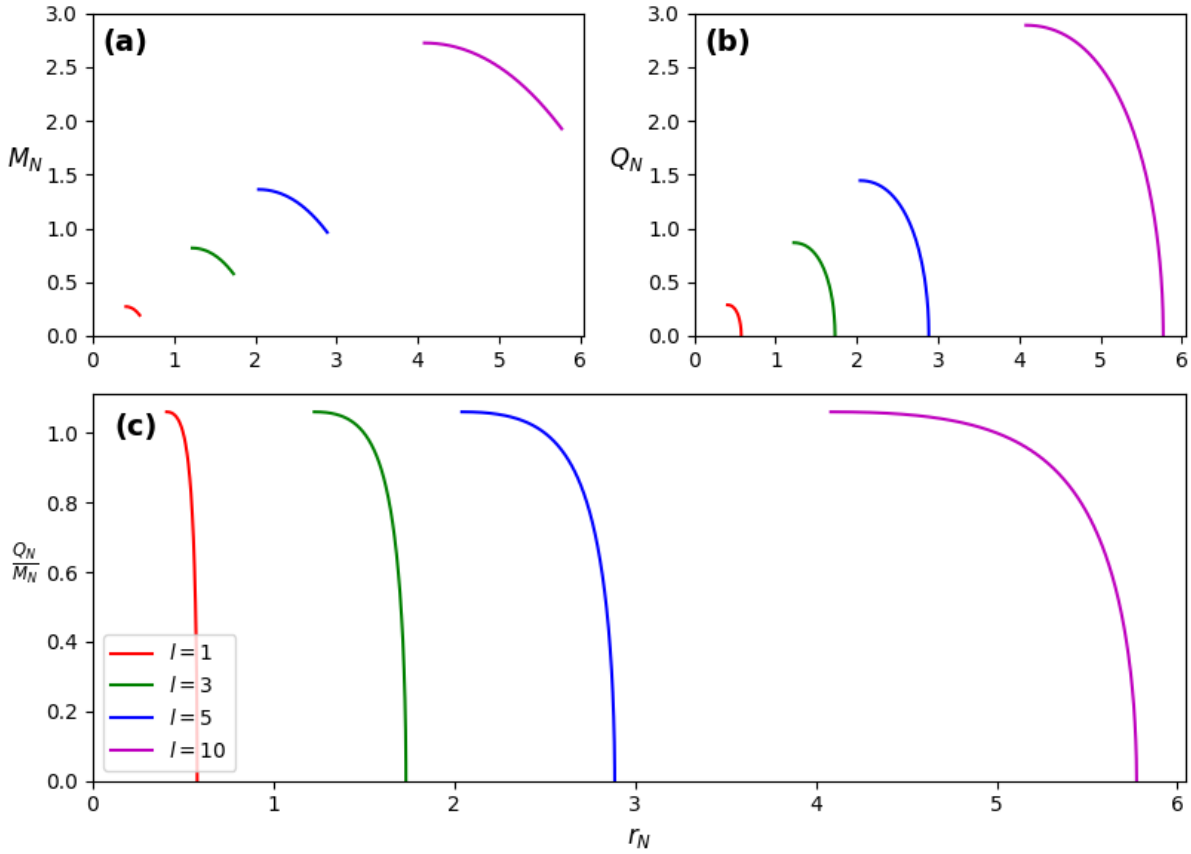

Figure 4.5: (a) Mass M_N, (b) charge Q_N, and (c) charge-to-mass ratio Q_N/M_N for a Nariai RNdS black hole as a function of the degenerate horizon radius r_N for different values of the cosmological constant. Note that r_N actually *in*creases as M_N and Q_N decrease, since the cosmological horizon can relax outward as the black hole becomes less heavy.

situations. Thus, these findings call for a more careful implementation of the numerical solver in future work. It would also be useful to have an explicit calculation of the one-loop determinant for these more complex spacetimes. Moreover, we have in no way incorporated into our analysis [37]'s intuition that the black hole's charge and mass should receive significant corrections in the adiabatic regime due to the production of charged particles outside of the cosmological horizon, an important remark that definitely deserves more attention in later work. Finally, we have only briefly touched on the subject of the ultra-cold RNdS configuration in this thesis. However, since it lies at the intersection of the extremal and Nariai branches of the RNdS phase space, it could be an extremely interesting and singular object of study.

Conclusion

In this thesis, we saw how, if there exists at least one particle species that breaks the FL bound, i.e. for which $m^2 < qgM_PH$, the Schwinger effect causes RNdS black holes to shed their charge in an explosive fashion, leaving behind an electrically neutral black hole with a mass that is higher than that allowed in a dS background. This causes the spacetime to be devoured in a Big Crunch, a pathology that, intuitively, should be avoided by putting a lower bound on the mass of charged particles. Thus, considering the semi-classical evolution of different kinds of black holes can lead to interesting new insights into parts of physics that one would not immediately associate with black hole physics.

Still, some doubts exist about the assumptions that went into the derivation of the FL bound. Therefore, we have made a contribution towards a better picture of the spatial profile of the Schwinger rate in extremal and Nariai RNdS spacetimes, since understanding the interplay between the produced particle cloud and the cosmological horizon might be essential to reach a verdict on the validity of the FL bound. We found that the algorithm used for this task gave good results in the case of small extremal black holes (relative to the cosmological horizon), but performed worse for larger extremal black holes and for charged Nariai black holes. In future work, a more careful implementation of the numerical solver should be found, with special attention to possible instabilities near the cosmological horizon. Additionally, it would be good to have an explicit calculation of the one-loop determinant in these more complex cases.

All in all, the study of these extreme black hole spacetimes has turned out to be rather fruitful, even if we have no reason to expect to observe them in our universe anytime soon. Despite the often strict interpretation of the scientific methodology in terms of experiments, observations, and models, no one really knows where the next breakthrough will come from, and so we should remain open-minded about the more unorthodox approaches to fundamental physics. After all, new knowledge in physics, as any knowledge, always starts with a flash of imagination.

Appendix A

Worldline action expansion

In generic spacetimes, $R \neq 0$, so we have to include it in our expressions. However, in our model, we neglect backreactions of the quantum field on the spacetime, so we can set derivatives of R to zero. For completeness and with future work involving a dynamical cosmological constant in mind, we add such terms in our expansion anyway. The worldline action is given by

$$S_{\mathrm{wl}}[s,x] = \int_0^1 \mathrm{d}T \left(\frac{1}{4s} g_{\mu\nu}\dot{x}^\mu \dot{x}^\nu + eA_\mu \dot{x}^\mu + s\left(m^2 + \xi R\right) \right), \tag{A.1}$$

which we want to expand up to second order in s and x. To do so, we take $\dot{x}^\mu \to \dot{x}^\mu + \delta\dot{x}^\mu$ and $s \to s + \delta s$, expand $g_{\mu\nu}$, A_μ, and R:

$$\begin{aligned} g_{\mu\nu}(x+\delta x) &= g_{\mu\nu}(x) + g_{\mu\nu,\rho}(x)\delta x^\rho + \frac{1}{2} g_{\mu\nu,\rho\sigma}(x)\delta x^\rho \delta x^\sigma + \dots \\ A_\mu(x+\delta x) &= A_\mu(x) + A_{\mu,\nu}(x)\delta x^\nu + \frac{1}{2} A_{\mu,\nu\rho}(x)\delta x^\nu \delta x^\rho + \dots \\ R(x+\delta x) &= R(x) + R_{,\mu}(x)\delta x^\mu + \frac{1}{2} R_{,\mu\nu}(x)\delta x^\mu \delta x^\nu + \dots, \end{aligned} \tag{A.2}$$

and calculate each term in the worldline action up to second order.

The expansion of the worldline action is then given by

$$
\begin{aligned}
S^{(0)} &= \int_0^1 \mathrm{d}T \left(\frac{\tilde{m}^2}{4s} \dot{x}_\mu \dot{x}^\mu + eA_\mu \dot{x}^\mu + s \right) \\
S_s^{(1)} &= \int_0^1 \mathrm{d}T \left(1 - \frac{\tilde{m}^2}{4s^2} \dot{x}_\mu \dot{x}^\mu \right) \delta s \\
S_{ss}^{(2)} &= \int_0^1 \mathrm{d}T \, \delta s \frac{\tilde{m}^2}{4s^3} \dot{x}_\mu \dot{x}^\mu \delta s \\
S_{sx}^{(2)} &= \int_0^1 \mathrm{d}T \, \delta s \left(\frac{\tilde{m}^2}{2s^2} \frac{D^2 x_\mu}{\mathrm{d}T^2} + \xi R_{,\mu} \right) \delta x^\mu \\
S_x^{(1)} &= \int_0^1 \mathrm{d}T \left(-\frac{\tilde{m}^2}{2s} \frac{D^2 x_\mu}{\mathrm{d}T^2} + eF_{\mu\nu} \frac{Dx^\nu}{\mathrm{d}T} + \xi R_{,\mu} \right) \delta x^\mu \\
S_{xx}^{(2)} &= \int_0^1 \mathrm{d}T \, \delta x^\mu \left(\frac{\tilde{m}^2}{4s} \left[-g_{\mu\nu} \frac{\mathrm{d}^2}{\mathrm{d}T^2} - g_{\mu\rho,\nu} \ddot{x}^\rho - 2\dot{x}_\rho \Gamma^\rho_{\mu\nu} \frac{\mathrm{d}}{\mathrm{d}T} - g_{\mu\rho,\nu\sigma} \dot{x}^\sigma \dot{x}^\rho + \frac{1}{2} g_{\sigma\rho,\mu\nu} \dot{x}^\sigma \dot{x}^\rho \right] \right. \\
&\qquad \left. + \frac{e}{2} \left[F_{\mu\nu} \frac{\mathrm{d}}{\mathrm{d}T} + \left(A_{\rho,\nu\mu} - A_{\mu,\nu\rho} \right) \dot{x}^\rho \right] + \frac{1}{2} \xi R_{,\mu\nu} \right) \delta x^\nu .
\end{aligned}
\tag{A.3}
$$

Bibliography

[1] L. Aalsma, J. P. van der Schaar, and M. Visser, "Extremal Black Hole Decay in de Sitter Space", arXiv pre-print (2024).

[2] B. P. Abbott et al. (LIGO Scientific Collaboration and Virgo Collaboration), "Observation of Gravitational Waves from a Binary Black Hole Merger", Phys. Rev. Lett. **116**, 061102 (2016).

[3] M. Abdul-Karim et al. (DESI Collaboration), "DESI DR2 Results II: Measurements of Baryon Acoustic Oscillations and Cosmological Constraints", arXiv pre-print (2025).

[4] K. Akiyama et al. (The Event Horizon Telescope Collaboration), "First M87 Event Horizon Telescope Results. I. The Shadow of the Supermassive Black Hole", ApJL **875**, L1 (2019).

[5] D. Anninos, "De Sitter Musings", Int. J. Mod. Phys. A **27**, 1230013 (2012).

[6] F. Bastianelli, J. M. Dávila, and C. Schubert, "Gravitational corrections to the Euler-Heisenberg Lagrangian", JHEP **2009**, article number 86 (2009).

[7] F. Bastianelli and A. Zirotti, "Worldline formalism in a gravitational background", Nucl. Phys. B **642**, 372–388 (2002).

[8] Z. Bern and D. A. Kosower, "Efficient calculation of one-loop QCD amplitudes", Phys. Rev. Lett. **66**, 1669–1672 (1991).

[9] N. D. Birrell and P. C. W. Davies, *Quantum Fields in Curved Space*, Cambridge Monographs on Mathematical Physics (Cambridge University Press, 1982).

[10] M. J. Blacker et al., "Quantum corrections to the path integral of near extremal de Sitter black holes", arXiv pre-print (2025).

[11] R. Bousso and S. W. Hawking, "(Anti-)evaporation of Schwarzschild-de Sitter black holes", Phys. Rev. D **57**, 2436–2442 (1998).

[12] A. R. Brown et al., "The evaporation of charged black holes", arXiv pre-print (2024).

[13] P. F. Byrd and M. D. Friedman, *Handbook of Elliptic Integrals for Engineers and Scientists*, 2nd ed., Grundlehren der mathematischen Wissenschaften (Springer-Verlag, 1971).

[14] S. M. Carroll, *Spacetime and Geometry: An Introduction to General Relativity* (Cambridge University Press, 2019).

[15] K. H. Choi, S. Hofmann, and M. Schneider, "Local diagnostic program for unitary evolution in general spacetimes", Phys. Rev. D **111**, 025019 (2025).

[16] T. D. Cohen and D. A. McGady, "Schwinger mechanism revisited", Phys. Rev. D **78**, 036008 (2008).

[17] S. Coleman, "The uses of instantons", in *Aspects of Symmetry: Selected Erice lectures of Sidney Coleman* (Cambridge University Press, Cambridge, 1985), pp. 265–350.

[18] P. A. M. Dirac, "The quantum theory of the electron", Proc. R. Soc. A **117**, 610–624 (1928).

[19] P. A. M. Dirac, "A theory of electrons and protons", Proc. R. Soc. A **126**, 360–365 (1930).

[20] P. A. M. Dirac, "Discussion of the infinite distribution of electrons in the theory of the positron", Math. Proc. Camb. Philos. Soc. **30**, 150–163 (1934).

[21] A. Einstein, "Näherungsweise Integration der Feldgleichungen der Gravitation", Sitzungsberichte der Königlich Preussischen Akademie der Wissenschaften, 688–696 (1916).

[22] R. P. Feynman, "Space-Time Approach to Non-Relativistic Quantum Mechanics", Rev. Mod. Phys. **20**, 367–387 (1948).

[23] R. P. Feynman, "Space-Time Approach to Quantum Electrodynamics", Phys. Rev. **76**, 769–789 (1949).

[24] A. Frizzo, L. Magnea, and R. Russo, "Scalar field theory limits of bosonic string amplitudes", Nucl. Phys. B **579**, 379–410 (2000).

[25] A. M. Ghez et al., "High Proper-Motion Stars in the Vicinity of Sagittarius A*: Evidence for a Supermassive Black Hole at the Center of Our Galaxy", ApJ **509**, 678–686 (1998).

[26] G. W. Gibbons, "Vacuum polarization and the spontaneous loss of charge by black holes", Commun. Math. Phys. **44**, 245–264 (1975).

[27] G. W. Gibbons and S. W. Hawking, "Action integrals and partition functions in quantum gravity", Phys. Rev. D **15**, 2752–2756 (1977).

[28] G. W. Gibbons and S. W. Hawking, "Cosmological event horizons, thermodynamics, and particle creation", Phys. Rev. D **15**, 2738–2751 (1977).

[29] S. Gillessen et al., "Monitoring Stellar Orbits Around the Massive Black Hole in the Galactic Center", ApJ **692**, 1075–1109 (2009).

[30] J. B. Hartle and S. W. Hawking, "Path-integral derivation of black-hole radiance", Phys. Rev. D **13**, 2188–2203 (1976).

[31] S. Hassan, G. Obied, and J. March-Russell, "De Sitter space constraints on brane tensions and couplings", JHEP **2025**, article number 221 (2025).

[32] S. W. Hawking, "Black hole explosions?", Nature **248**, 30–31 (1974).

[33] S. W. Hawking, "Particle creation by black holes", Commun. Math. Phys. **43**, 199–220 (1975).

[34] S. W. Hawking and G. F. R. Ellis, *The Large Scale Structure of Space-Time*, Cambridge Monographs on Mathematical Physics (Cambridge University Press, 2023).

[35] W. Heisenberg and H. Euler, "Folgerungen aus der Diracschen Theorie des Positrons", Z. Physik **98**, 714–732 (1936).

[36] J. Kevorkian and J. D. Cole, *Multiple Scale and Singular Perturbation Methods*, Applied Mathematical Sciences (Springer, 1996).

[37] P. Lin and G. Shiu, "Schwinger effect of extremal Reissner-Nordström black holes", JHEP **2025**, article number 17 (2025).

[38] M. Lüben, D. Lüst, and A. R. Metidieri, "The Black Hole Entropy Distance Conjecture and Black Hole Evaporation", Fortsch. Phys. **69**, 2000130 (2021).

[39] M. Montero and G. Shiu, "A Gentle Hike Through the Swampland", in *Handbook of Quantum Gravity*, edited by C. Bambi, L. Modesto, and I. Shapiro (Springer, Singapore, 2024).

[40] M. Montero, T. Van Riet, and G. Venken, "Festina Lente: EFT Constraints from Charged Black Hole Evaporation in de Sitter", JHEP **2020**, article number 39 (2020).

[41] M. Montero et al., "The FL bound and its phenomenological implications", JHEP **2021**, article number 9 (2021).

[42] H. Nariai, "On a New Cosmological Solution of Einstein's Field Equations of Gravitation", Gen. Relativ. Gravit. **31**, 963–971 (1999), reprint of a 1951 article in Scientific Reports of the Táhoku University.

[43] A. I. Nikishov, "Pair Production by a Constant External Field", Zh. Eksp. Teor. Fiz. **30**, 660–662 (1970).

[44] K. Osterwalder and R. Schrader, "Axioms for Euclidean Green's functions II", Commun. Math. Phys. **42**, 281–305 (1975).

[45] D. N. Page, "Particle emission rates from a black hole: Massless particles from an uncharged, nonrotating hole", Phys. Rev. D **13**, 198–206 (1976).

[46] D. N. Page, "Particle emission rates from a black hole. III. Charged leptons from a nonrotating hole", Phys. Rev. D **16**, 2402–2411 (1977).

[47] M. Paranjape, *The Theory and Applications of Instanton Calculations*, Cambridge Monographs on Mathematical Physics (Cambridge University Press, 2023).

[48] M. K. Parikh and F. Wilczek, "Hawking Radiation As Tunneling", Phys. Rev. Lett. **85**, 5042–5045 (2000).

[49] R. Penrose, "Gravitational Collapse and Space-Time Singularities", Phys. Rev. Lett. **14**, 57–59 (1965).

[50] R. Penrose, "Gravitational Collapse: The Role of General Relativity", Gen. Relativ. Gravit. **34**, 1141–1165 (2002), reprint of a 1969 article in Rivista del Nuovo Cimento.

[51] S. Perlmutter et al., "Measurements of Ω and Λ from 42 High-Redshift Supernovae", ApJ **517**, 565–586 (1999).

[52] P. C. Peters, "Perturbations in the Schwarzschild Metric", Phys. Rev. **146**, 938–946 (1966).

[53] J. Polchinski, "The Black Hole Information Problem", in New Frontiers in Fields and Strings (2017) Chap. 6, pp. 353–397.

[54] S. Raju, "Lessons from the Information Paradox", arXiv pre-print (2021).

[55] H. Reall, "Black Holes", Mathematical Tripos Part III, Lecture Notes (2024).

[56] A. G. Riess et al., "Observational Evidence from Supernovae for an Accelerating Universe and a Cosmological Constant", AJ **116**, 1009–1038 (1998).

[57] L. J. Romans, "Supersymmetric, cold and lukewarm black holes in cosmological Einstein-Maxwell theory", Nucl. Phys. B **383**, 395–415 (1992).

[58] C. Schubert, "Perturbative quantum field theory in the string-inspired formalism", Phys. Rep. **355**, 73–234 (2001).

[59] M. D. Schwartz, *Quantum Field Theory and the Standard Model* (Cambridge University Press, 2013).

[60] J. Schwinger, "On Gauge Invariance and Vacuum Polarization", Phys. Rev. **82**, 664–679 (1951).

[61] T. P. Singh, "Gravitational collapse, black holes and naked singularities", J. Astrophys. Astron. **20**, 221–232 (1999).

[62] M. J. Strassler, "Field theory without Feynman diagrams: One-loop effective actions", Nucl. Phys. B **385**, 145–184 (1992).

[63] L. Susskind, "Entanglement and Chaos in De Sitter Space Holography: An SYK Example", JHAP **1**, 1–22 (2021).

[64] L. Verde, N. Schöneberg, and H. Gil-Marín, "A Tale of Many H_0", Annu. Rev. Astron. Astrophys. **62**, 287–331 (2024).

[65] R. M. Wald, *Quantum Field Theory in Curved Spacetime and Black Hole Thermodynamics*, Chicago Lectures in Physics (The University of Chicago Press, 1994).

[66] R. M. Wald, "Gravitational Collapse and Cosmic Censorship", in *Black Holes, Gravitational Radiation and the Universe: Essays in Honor of C.V. Vishveshwara*, edited by B. R. Iyer and B. Bhawal (Springer, Dordrecht, 1999), pp. 69–86.

[67] V. Weisskopf, "Über die Elektrodynamik des Vakuums auf Grund der Quantentheorie des Elektrons", Mat.-Fys. Medd. **14**, 1–39 (1936).

[68] M. F. Wondrak, W. D. van Suijlekom, and H. Falcke, "Gravitational Pair Production and Black Hole Evaporation", Phys. Rev. Lett. **130**, 221502 (2023).

[69] F. J. Zerilli, "Perturbation analysis for gravitational and electromagnetic radiation in a Reissner-Nordström geometry", Phys. Rev. D **9**, 860–868 (1974).

Institute for Theoretical Physics
Celestijnenlaan 200D box 2415
3001 LEUVEN, BELGI"E
tel. + 32 16 32 72 32
www.kuleuven.be